

# **NAVAL POSTGRADUATE SCHOOL MONTEREY, CALIFORNIA**



## **THESIS**



### **MODELING THE EFFECTS OF VARIATIONS AND ABSORPTION ON THE TRANSITION RADIATION PRODUCED FROM A STACK OF FOILS**

by

Nicholas J. Prins  
June, 1995

Thesis Advisor:

John R. Neighbours

Co-Advisor:

Fred R. Buskirk

19960118018

Approved for public release; distribution is unlimited.

DTIC QUALITY INSPECTED 3

REPORT DOCUMENTATION PAGE			Form Approved OMB No. 0704-0188
<p>Public reporting burden for this collection of information is estimated to average 1 hour per response, including the time for reviewing instruction, searching existing data sources, gathering and maintaining the data needed, and completing and reviewing the collection of information. Send comments regarding this burden estimate or any other aspect of this collection of information, including suggestions for reducing this burden, to Washington Headquarters Services, Directorate for Information Operations and Reports, 1215 Jefferson Davis Highway, Suite 1204, Arlington, VA 22202-4302, and to the Office of Management and Budget, Paperwork Reduction Project (0704-0188) Washington DC 20503.</p>			
1. AGENCY USE ONLY ( <i>Leave blank</i> )	2. REPORT DATE June 1995	3. REPORT TYPE AND DATES COVERED Masters Thesis	
4. TITLE AND SUBTITLE  MODELING THE EFFECTS OF VARIATIONS AND ABSORPTION ON THE TRANSITION RADIATION PRODUCED FROM A STACK OF FOILS		5. FUNDING NUMBERS	
6. AUTHOR(S) Nicholas J. Prins			
7. PERFORMING ORGANIZATION NAME(S) AND ADDRESS(ES) Naval Postgraduate School Monterey CA 93943-5000		8. PERFORMING ORGANIZATION REPORT NUMBER	
9. SPONSORING/MONITORING AGENCY NAME(S) AND ADDRESS(ES)		10. SPONSORING/MONITORING AGENCY REPORT NUMBER	
11. SUPPLEMENTARY NOTES The views expressed in this thesis are those of the author and do not reflect the official policy or position of the Department of Defense or the U.S. Government.			
12a. DISTRIBUTION/AVAILABILITY STATEMENT Approved for public release; distribution is unlimited.		12b. DISTRIBUTION CODE	
13. ABSTRACT  Modeling transition radiation is a method to simulate the radiation produced by a relativistic charged particle passing through a stack of foils when variables such as foil thickness, interfoil spacing, number of cells, beam energy, and absorption change from an idealized case. The results of the modeling show how rapidly the radiation intensity produced by a relativistic charged particle in the foil stack decreases as randomness in foil thickness and spacing increase and can be used to establish practical tolerances for stack design. Including the effect of photon absorption by the foils will give a realistic radiation intensity for a particular material. The choice of foil material will determine the level of energy below which the photon energy is strongly absorbed. Modeling the effect of absorption in certain foil materials also indicates the x-ray absorption K edge can be used to isolate particular energies and angles of photon emission.			
14. SUBJECT TERMS Transition Radiation, X-Rays, Linear Accelerator			15. NUMBER OF PAGES 87
			16. PRICE CODE
17. SECURITY CLASSIFICATION OF REPORT Unclassified	18. SECURITY CLASSIFICATION OF THIS PAGE Unclassified	19. SECURITY CLASSIFICATION OF ABSTRACT Unclassified	20. LIMITATION OF ABSTRACT UL



**Approved for public release, distribution is unlimited**

**MODELING THE EFFECTS OF VARIATIONS AND ABSORPTION ON THE  
TRANSITION RADIATION PRODUCED FROM A STACK OF FOILS**

Nicholas J. Prins  
Captain, United States Army  
B.S., Hope College, Holland, Michigan, 1985

Submitted in partial fulfillment of the  
requirements for the degree of

**MASTER OF SCIENCE IN PHYSICS**

from the

**NAVAL POSTGRADUATE SCHOOL**  
**June 1995**

Author: Nicholas J. Prins

Nicholas J. Prins

Approved by: John R. Neighbours

John R. Neighbours, Thesis Advisor

Fred R. Buskirk

Fred R. Buskirk, Co-Advisor

W.B. Colson

William B. Colson, Chairman, Department of Physics



## ABSTRACT

Modeling transition radiation is a method to simulate the radiation produced by a relativistic charged particle passing through a stack of foils when variables such as foil thickness, interfoil spacing, number of cells, beam energy, and absorption change from an idealized case. The results of the modeling show how rapidly the radiation intensity produced in the foil stack decreases as randomness in foil thickness and spacing increase and can be used to establish practical tolerances for stack design. Including the effect of photon absorption by the foils will give a realistic radiation intensity for a particular material. The choice of foil material will determine the level of energy, below which the photon energy is strongly absorbed. Modeling the effect of absorption in certain foil materials also indicates the x-ray absorption K edge can be used to isolate particular energies and angles of photon emission.

Accesion For	
NTIS	CRA&I <input checked="" type="checkbox"/>
DTIC	TAB <input type="checkbox"/>
Unannounced <input type="checkbox"/>	
Justification _____	
By _____	
Distribution / _____	
Availability Codes	
Dist	Avail and / or Special
A-1	



## TABLE OF CONTENTS

I. INTRODUCTION .....	1
II. TRANSITION RADIATION .....	3
III. IDEALIZED THIN FOIL STACKS .....	5
IV. MODELING THE FOIL STACK.....	11
V. MODELING VARIATIONS FOR A STACK OF FOUR FOILS.....	17
VI. EFFECT OF ABSORPTION.....	31
VII. SELECTION OF PARAMETERS WHICH PLACE INTENSITY PEAK AT A DESIRED ENERGY AND ANGLE.....	43
VIII. CONCLUSIONS AND FUTURE WORK .....	51
APPENDIX A. ABSORPTION CONSTANTS.....	53
APPENDIX B. MAXIMUM INTENSITIES.....	55
APPENDIX C. COMPUTER PROGRAMS.....	57
LIST OF REFERENCES .....	73
INITIAL DISTRIBUTION LIST .....	75



## **ACKNOWLEDGMENT**

The author would like to thank Professor John Neighbours and Professor Fred Buskirk for their commitment, patience, and professionalism. Their decision to accept me as a thesis student, even in their retirement, has made this thesis a rewarding and learning experience for me. May they both live as long as they want and never want as long as they live.



## I. INTRODUCTION

The interaction of a relativistic charged particle with the medium which it transverses may lead to the generation of Cherenkov radiation, which is broad banded and dependent on the length of the interaction path. The mechanism is the acceleration of the molecules of the medium in the vicinity of the charged particle.

Transition radiation consists of photons generated by an energetic charged particle transversing an interface between two media. If the dielectric constant has a spatial discontinuity, as in the interface between two different media, a charged particle experiencing this sudden change produces transition radiation. Unlike Cherenkov radiation, where radiation is produced only when the particle velocity exceeds the phase velocity of light in the direction of the particle; for transition radiation this velocity matching is not necessary.[Ref. 1] Also, transition radiation always has an angular spread, where Cherenkov radiation may be confined to a small angular cone in the direction of the particle.

In the case of a single slab or foil, transition radiation will be produced by each interface, ie. both sides, as the charged particle passes through. Transition radiation is rather low intensity and to increase the radiation intensity, multiple foils may be used. With the correct foil thickness and interfoil spacing, the transition radiation produced by each foil can be added coherently as in Fig. 1, analogous to an optical diffraction grating, to greatly increase the intensity.[Ref. 2] Figure 1 shows two such rays emitted at the angle  $\theta$ .

Transition radiation has been the subject of many papers, primarily for an idealized case where the foil thickness and spacing described above are exact throughout the multiple foils. Some authors consider the case to be idealized as long as the deviation in the foil thickness,  $\Delta_1$ , and the deviation in spacing,  $\Delta_2$ , satisfy the inequalities

$$\Delta_1 \ll \frac{z_1}{\sqrt{2N}},$$

and

$$\Delta_2 \ll \frac{z_2}{\sqrt{2N}},$$

where  $z_{1,2}$  are the formation lengths, a quantity to be defined later, and  $N$  is the number of foils.[Ref. 1] This paper will address (1) the production of transition radiation for the ideal case; (2) the effects of variations in foil thickness and spacing; (3) the effects of absorption for different materials; and (4) discuss what limits and considerations should be taken into account for designing foil stacks for different materials.

Transition radiation has several possible applications. One application is in particle identification and energy measurements. Transition radiation is analogous to Cherenkov radiation and could possibly replace existing Cherenkov detectors. Transition radiation could also be used for threshold detectors for detecting particles with energies above a given value or in particle beam diagnostics, to accurately measure the beam energy and identify the type of particle. Another possible application is as a source enhancement. A foil stack can be used to increase the spectral brightness (photons per unit solid angle per unit area of source) of a transition radiation source[Ref. 1].

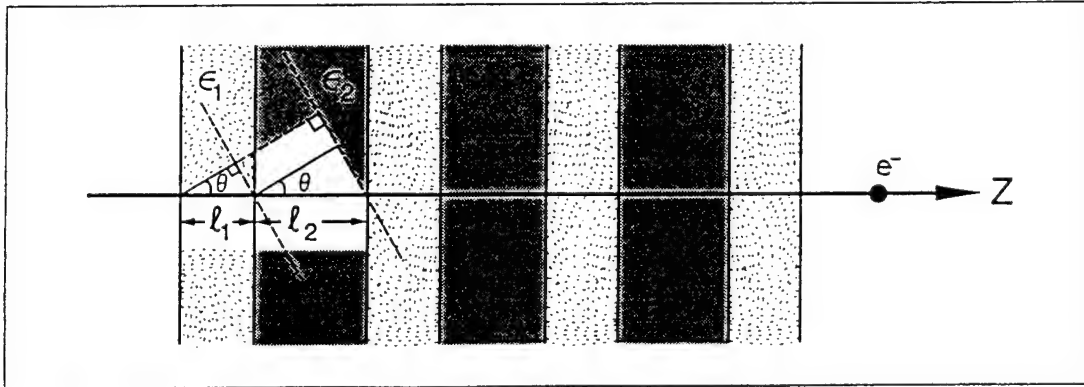


Fig. 1 Transition radiation from a periodic medium with uniform spacing. If the phase of the emitted radiation varies by  $2\pi n$  ( $n$  an integer) for each foil interface, the radiation adds in phase and the intensity varies as the square of the number of foils.[Ref. 1]

## II. TRANSITION RADIATION

At the interface the charged particle will interact over a set distance, called the formation length, given by

$$z_i = \frac{2c}{\omega \left[ 1 - \beta (\varepsilon_i - \sin^2 \theta)^{\frac{1}{2}} \right]}, \quad (1)$$

where  $\omega$  is the angular frequency of the radiation,  $\theta$  is the angle of emission,  $\omega_i$  is the respective plasma frequency of the medium,  $c$  is the speed of light in a vacuum and

$$\varepsilon_i = 1 - \left( \frac{\omega_i}{\omega} \right)^2$$

is the permittivity of the medium,  $\beta = v/c$ , and  $\gamma = (1 - \beta^2)^{\frac{1}{2}}$ . Considering a small emission angle and a foil in a vacuum, the formation lengths become,

$$z_1 = \frac{2\lambda}{\pi} \left( \frac{1}{\gamma^2} + \theta^2 + \left( \frac{\omega_i}{\omega} \right)^2 \right)^{-1}, \quad (2)$$

for the foil and,

$$z_2 = \frac{2\lambda}{\pi} \left( \frac{1}{\gamma^2} + \theta^2 \right)^{-1}, \quad (3)$$

for the vacuum since there is no plasma frequency for vacuum.

Transition radiation can conveniently be considered as the product of several factors.  $F_1$  is the contribution from a single interface. It describes the photons produced as an electron crosses a single boundary between two different media and is given by:

$$F_1 = \frac{\alpha \omega \sin^2 \theta}{16\pi^2 c^2} (z_1 - z_2)^2, \quad (4)$$

where  $\alpha$  is the fine structure constant. The coherent superposition of radiation from the two surfaces of a single foil is another factor given by

$$F_2 = 4 \sin^2 Y, \quad (5)$$

where

$$Y = \frac{l_1}{z_1}, \quad (6)$$

and  $l_1$  is the foil thickness.

For  $N$  equally spaced foils of identical thickness in a vacuum, the number of photons per frequency per solid angle is given by:

$$\frac{d^2 N}{d\omega d\Omega} = F_1 F_2 F_3. \quad (7)$$

The third factor  $F_3$  gives the summation of the contribution of each foil in the stack.

For  $N$  foils,  $F_3$  has the form:

$$F_3 = \frac{\sin^2 NX}{\sin^2 X}, \quad (8)$$

where,

$$X = \frac{l_1}{z_1} + \frac{l_2}{z_2}, \quad (9)$$

and  $l_1$  is the foil thickness and  $l_2$  is the vacuum spacing. [Ref. 2]

These equations assume  $N$  idealized foils with no reflections or absorption of photons or particles. By idealized, it is meant that the thickness and spacing of foils is exact and precise; there is no variation in either the spacing or foil thickness.

### III. IDEALIZED THIN FOIL STACKS

In the preceding chapter, the equations were developed for the radiation produced by an electron transversing a foil in a vacuum. The foil stack that will be referred to throughout this paper consists of  $N$  foils separated by a vacuum spacing. The foil stack is considered to be made so that there are  $N$  cells where each cell is a foil and vacuum spacing. The mechanics of making the stack is difficult only because of the small sizes and tolerances required. Future chapters will discuss these tolerances further. Equation 7 shows that the distribution of transition radiation is the product of three factors,  $F_1$ ,  $F_2$ , and  $F_3$ . It is convenient to discuss each of these factors in order.

For  $F_1$  there is an angle,  $\theta_i$ , that maximizes the function, which is to a first order approximation,

$$\theta_i \approx \left[ \frac{1}{\gamma^2} + \left( \frac{\omega_2}{\omega} \right)^2 \right]^{\frac{1}{2}}, \quad (10)$$

where  $\omega_2$  is the plasma frequency of the medium surrounding the foil. For a foil in vacuum, Eq. 10 reduces to the rule of thumb,  $\theta_i = 1/\gamma$ . For example, an electron beam of 855 MeV has an  $\theta_i$  value of 0.5 mrad. Thus for a foil in vacuum, the relatively broad maximum of  $F_1$  is determined only by the value of  $\gamma$ . For this reason, this paper concentrates on the role of  $F_2$  and  $F_3$  in determining the photon emission given by Eq. 7. This is appropriate since  $F_1$  is relatively slowly varying.

From Eq. 6,  $F_2$  will have a maximum value of 4 for odd integer values of  $s$ . So,

$$Y = s \frac{\pi}{2} \quad \text{for } s=1,3,5,\dots$$

Similarly, from Eq. 8, which is the optical grating equation,  $F_3$  will have a maximum for  $X = r\pi$  for  $r=1,2,3\dots$ .

The maximum value of  $F_3$  will be  $N^2$  at integer values of  $r$ , and the maximum value of  $F_2 F_3$  is  $4N^2$  for integer values of  $r$  and odd integer values of  $s$ . [Ref. 1]

These conditions may be plotted for a specific case. With the photon energy  $E = \hbar\omega$  ranging from 0 to 10 keV and the emission angle  $\theta$  ranging from 0 to 2 mrad, the calculated results for a stack of 4 equally spaced foils are plotted in Fig. 2. The solid lines represent odd integer values of  $s$  or maximas of  $F_2$  and the dotted lines represent integer values of  $r$  or maximas of  $F_3$ . Intensity peaks are expected to occur for the values of  $E$  and  $\theta$  where the solid and dotted lines intersect. A corresponding plot of the radiation intensity is plotted in Fig. 3. The maximums of Fig. 3 are where the predictions of Fig. 2 show, the intersections of the  $r$  and  $s$  lines.

The maximum value of the contour plot, Fig. 3, occurs for the  $r=1, s=1$  intersection. Each contour in the figure has a value of 20 and the maximum for four foils is 64. From this maximum, at this particular energy and angle, the intensity tapers off as the energy and angle are changed.

Additional foils have the obvious effect of increasing the intensity, which varies as  $4N^2$ . But, additional foils also have effect of sharpening the intensity contour to a narrower angle, much as an optical grating with more slits tends to intensify the image. A plot with the same values as Fig. 3 except for a stack of 8 foils demonstrates this in Fig. 4.

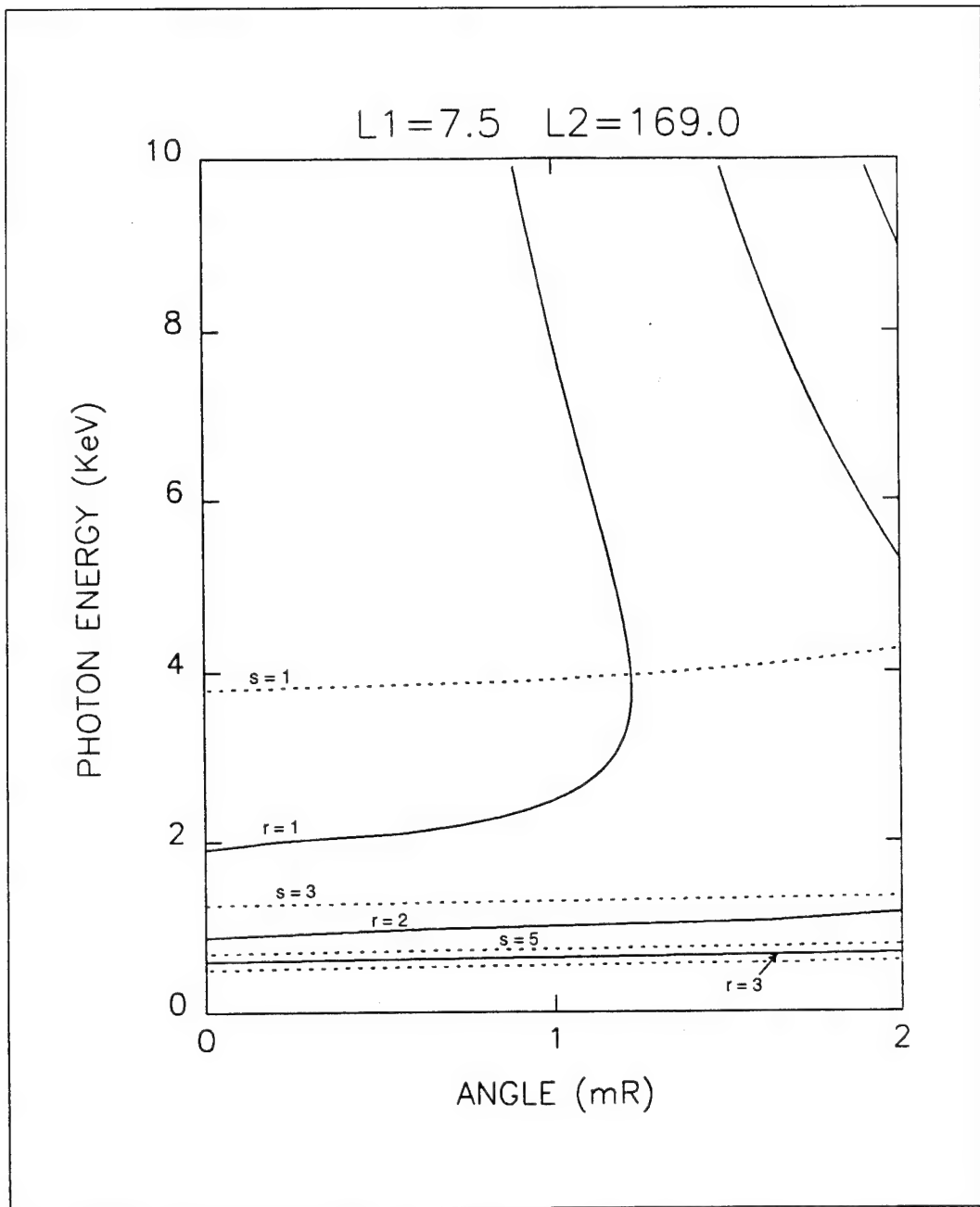


Fig. 2 With  $l_1 = 7.5 \mu\text{m}$ ,  $l_2 = 169 \mu\text{m}$ , and 4 Kapton foils, the maximum of the function  $F_2$  is represented by the dashed line. The maximum of the function  $F_3$  is represented by the solid lines. In both cases, the lowest order resonance are the top lines. Intersections maximize the product  $F_2 F_3$ .

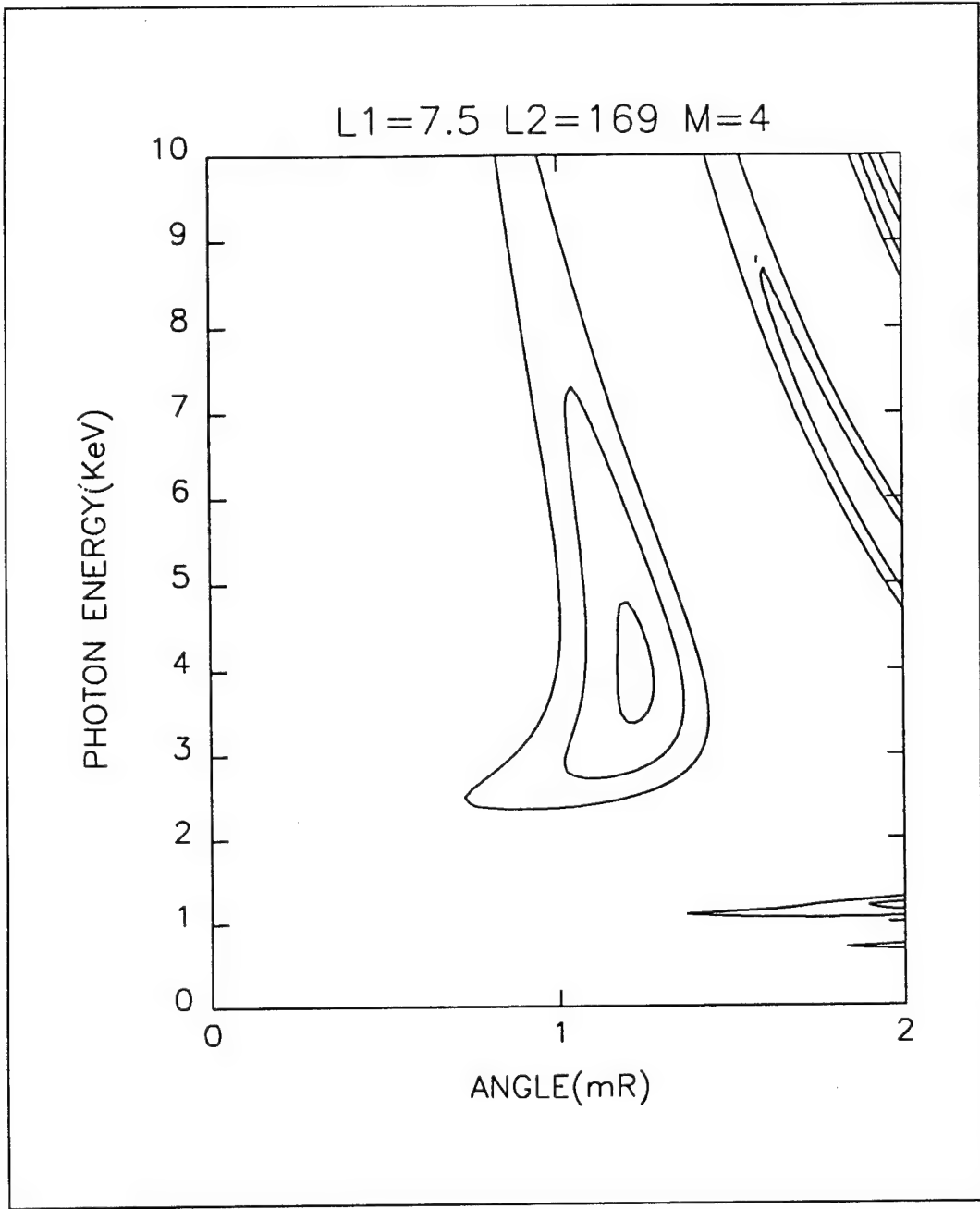


Fig. 3 Radiation intensity contours for the product  $F_2F_3$  with 4 Kapton foils,  $L_1 = 7.5 \mu\text{m}$ ,  $L_2 = 169 \mu\text{m}$ , maximum intensity = 63.972.

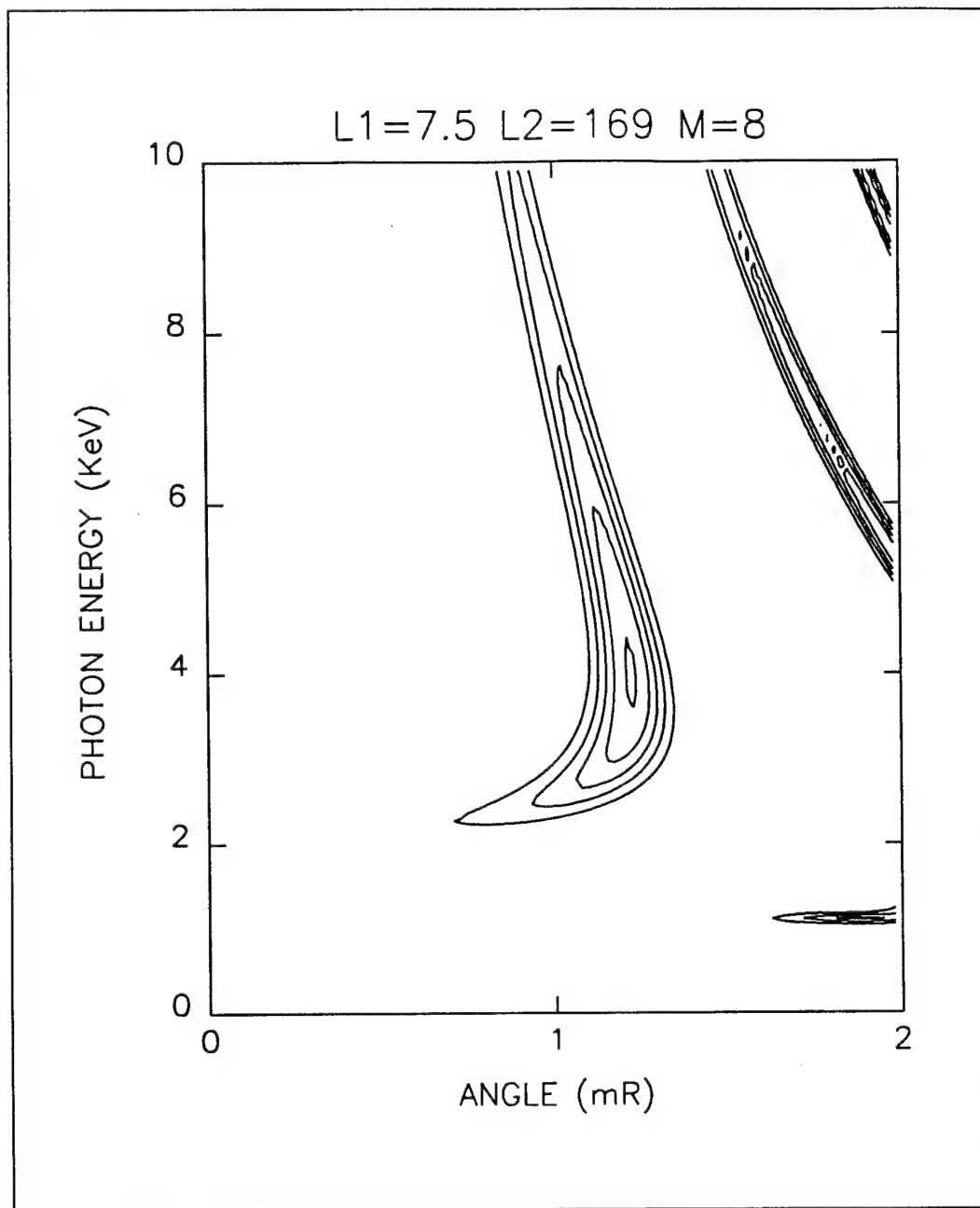


Fig. 4 Radiation intensity contours for the product  $F_2F_3$  with 8 Kapton foils,  $L_1 = 7.5 \mu\text{m}$ ,  $L_2 = 169 \mu\text{m}$ . Energy range of main maximum is the same compared the Fig. 3, but the angular width is narrower. Maximum intensity = 255.72



## IV. MODELING THE FOIL STACK

The use of Eq. 5 and Eq. 8 is a convenient method for studying the radiation pattern. However, these equations are for an ideal case. If the foil thickness and spacing have variations, another method must be used to calculate the radiation pattern.

The next step is to develop an algorithm to simulate each of the factors producing transition radiation as the variables of foil thickness and spacing are changed. Since the first factor,  $F_1$ , is independent of length and spacing, we will concentrate on the algorithm for simulating  $F_2$  and  $F_3$ . In the study of idealized thin foils, the factors  $F_2$  and  $F_3$  were derived for the case of no variation. To study the effects of variations, consider the sum

$$\left| \sum_{m=0}^{N-1} e^{iA_m} \{1 - e^{i\delta_m}\} \right|^2, \quad (11)$$

where

$$A_m = -\varphi \sum_{k=m+2}^N a_k - \varphi_0 \sum_{k=m+2}^N b_{k-1}, \quad (12)$$

and

$$\delta_m = -\varphi a_{m+1}. \quad (13)$$

The sum is over the  $N$  cells of the stack, where the foil thickness and spacing of the  $k$ th cell are given by  $a_k$  and  $b_k$  respectively. [Ref. 3] The constants  $\varphi$  and  $\varphi_0$  are yet to be defined.

To show how Eq. 11 reduces to the factors given in the idealized case, again consider the case of no variation so that  $a_k = a$ ,  $b_k = b$ . Eq. 12 and 13 then reduce to

$$A_m = -\varphi(N-m+2)a - \varphi_0(N-m+2)b,$$

and  $\delta_m = -\varphi a$ .

Inserting these values into Eq. 11, before taking the absolute value squared, one obtains,

$$\begin{aligned}
\sum_{m=0}^{N-1} e^{iA_m} \{1 - e^{i\delta_m}\} &= \sum_{m=0}^{N-1} e^{i[-\varphi a(N-m+2) - \varphi_0 b(N-m+2)]} [1 - e^{i\varphi a}], \\
&= [1 - e^{i\varphi a}] \sum_{m=0}^{N-1} e^{-i\varphi a(N-m+2)} e^{-i\varphi_0 b(N-m+2)}, \\
&= [1 - e^{i\varphi a}] e^{-i\varphi a(N+2)} e^{-i\varphi_0 b(N+2)} \sum_{m=0}^{N-1} e^{i(\varphi a + \varphi_0 b)m}.
\end{aligned} \tag{14}$$

Now, let  $R = \varphi a + \varphi_0 b$ , in which case the right hand side of Eq. 14 reduces to

$$\begin{aligned}
[1 - e^{i\varphi a}] e^{-i\varphi a(N+2)} e^{-i\varphi_0 b(N+2)} \left( \frac{1 - e^{iRN}}{1 - e^{iR}} \right) &= [1 - e^{i\varphi a}] e^{-i(N+2)R} e^{iRN/2} e^{-iR/2} \frac{\sin(R/2)}{\sin(NR/2)}, \\
&= [1 - e^{i\varphi a}] e^{-iR\left(\frac{N+3}{2}\right)} \frac{\sin(R/2)}{\sin(NR/2)}, \\
&= 2ie^{i\varphi a/2} \left[ \sin \frac{\varphi a}{2} \right] e^{-iR\left(\frac{N+3}{2}\right)} \frac{\sin(R/2)}{\sin(NR/2)}.
\end{aligned}$$

Thus, the summation in Eq. 11 becomes,

$$\sum_{m=0}^{N-1} e^{iA_m} \{1 - e^{i\delta_m}\} = 2ie^{i\varphi a/2} \left[ \sin \frac{\varphi a}{2} \right] e^{-iR\left(\frac{N+3}{2}\right)} \frac{\sin(R/2)}{\sin(NR/2)}, \tag{15}$$

Now, taking the square of the absolute value,

$$\left| \sum_{m=0}^{N-1} e^{iA_m} \{1 - e^{i\delta_m}\} \right|^2 = 4 \sin^2 \left( \frac{\varphi a}{2} \right) \frac{\sin^2(R/2)}{\sin^2(NR/2)} \tag{16}$$

which is the same as  $F_2 F_3$  if  $Y = \varphi a / 2$  and  $X = R / 2$ . This procedure defines the constants  $\varphi = 2 / z_1$  and  $\varphi_0 = 2 / z_2$ . As a further check, an intensity plot from this summation is shown in Fig. 5 for the same values as Fig. 3. As expected from this derivation, the two figures are identical. This similarity says that Eq. 11 is adding the phase of the photons and the interference produced by the various cell foils together. Whether the interference is constructive, like an optical grating, or destructive will show in the result of the left hand side of Eq. 16. This is the algorithm to use for the case where foil thickness and spacing are not ideal.

Now that an algorithm for finding the intensity has been established, consider the effects of letting variations occur in the cell. To do this, a quantity called percent randomness, which is defined as a random number in the range of that value plus or minus the percent times the value, is used. For example, a ten percent randomness in  $I_1$  would be a random number falling within the range  $I_1 \pm 0.1I_1$ .

In creating the model, the intensity is averaged for a more consistent result. If the summation is done for just one particular random value, the intensity could be a higher or lower value than a statistical average, depending on what the actual random values are. To determine the statistical average, the result of  $M$  summations is added together and the answer is divided by  $M$  to obtain an average. This computation is carried out for every calculated point in the selected range of  $E$  and  $\theta$ . Depending on the values of each particular cell, the intensity will have a value for a particular  $E$  and  $\theta$ . If these values are the same for each random cycle, the average intensity will be close to the intensity calculated from a single cycle. If the intensity varies from cycle to cycle, the average intensity could be quite different from the intensity for each cycle.

This gives rise to the question of how many cycles to average over. In doing this average, the results from 10, 20 and 100 cycles were considered. To complete 100 cycles took the computer 4.5 days while 10 cycles took 2.5 hours. It turned out that the average converged very quickly, the difference in the maximum intensity between 10 and 100 cycles was less than 0.25. Plots to compare the difference between 10 and 100 cycles are shown in Fig. 6 and Fig. 7 respectively. Since there is essentially no difference, 10 cycles were used for all calculations.

Another consideration is the random number that is used in each cycle. To make a truly random number each cycle, and thereby obtain better averages, the random function requires a different seed or start point to generate the random number. The random function on the computer which was used took the number of seconds past midnight on the internal clock as the seed number. Since this number would always be different for each cycle, the numbers are considered random.

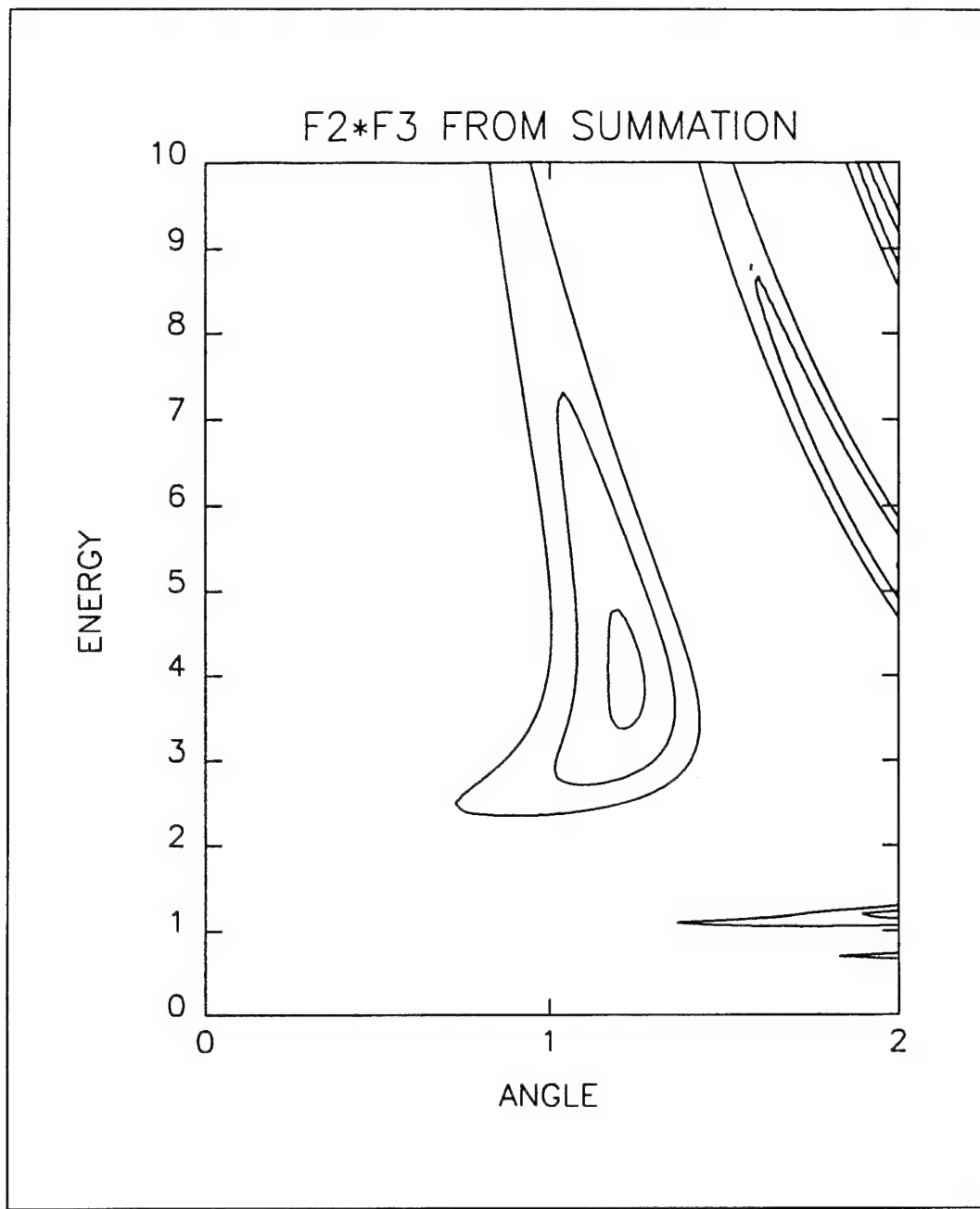


Fig. 5 Result of Eq. 11 for the product  $F_2F_3$  with 4 Kapton foils,  $l_1 = 7.5 \mu\text{m}$ ,  $l_2 = 169 \mu\text{m}$ . Compared to Fig. 3 the result is exactly the same. Maximum intensity = 63.972.

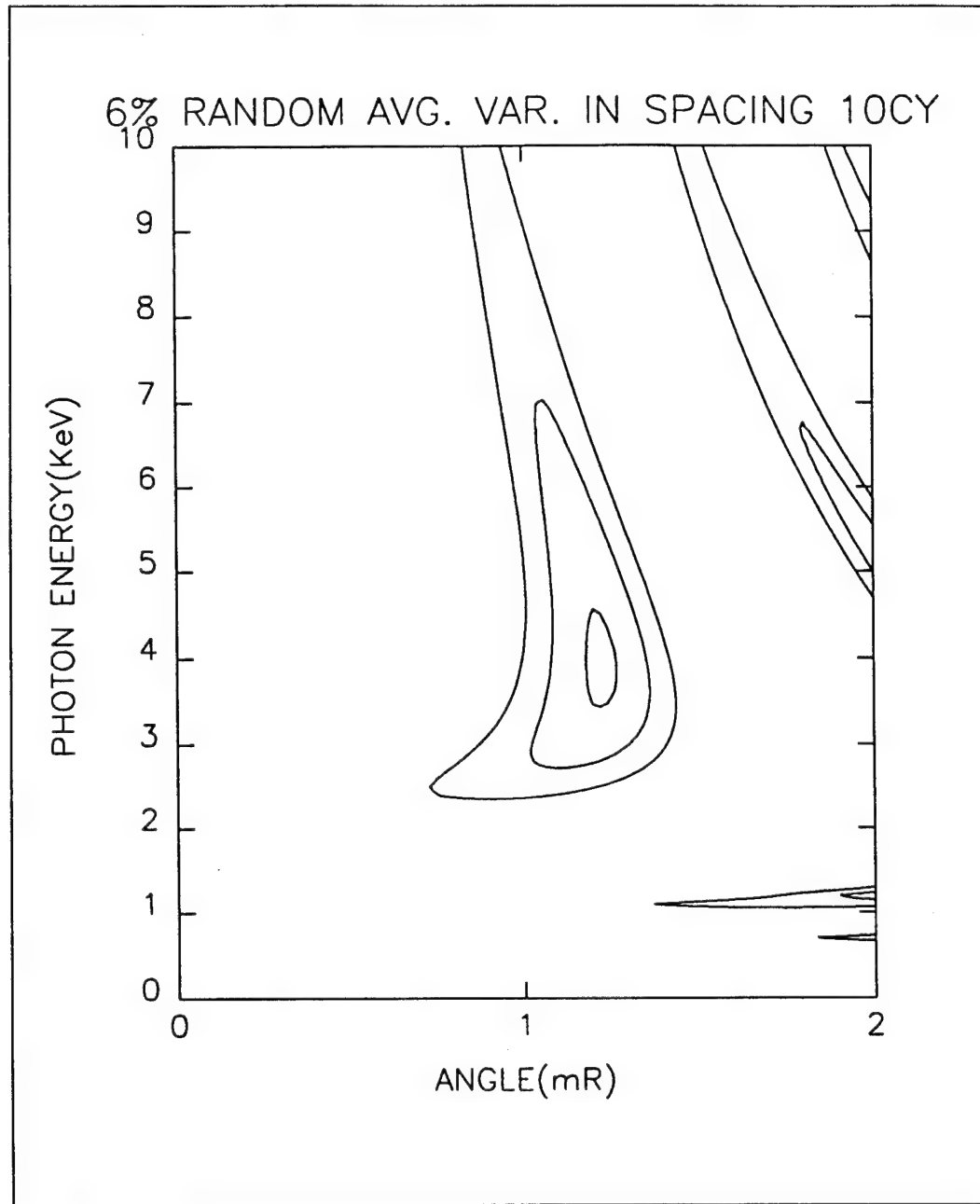


Fig. 6 Modeling the product  $F_2F_3$  with 4 Kapton foils,  $l_1 = 7.5 \mu\text{m}$ ,  $l_2 = 169 \mu\text{m}$ , for 10 cycles to calculate an average which is shown above. Maximum intensity = 62.610. 6% randomness in spacing.

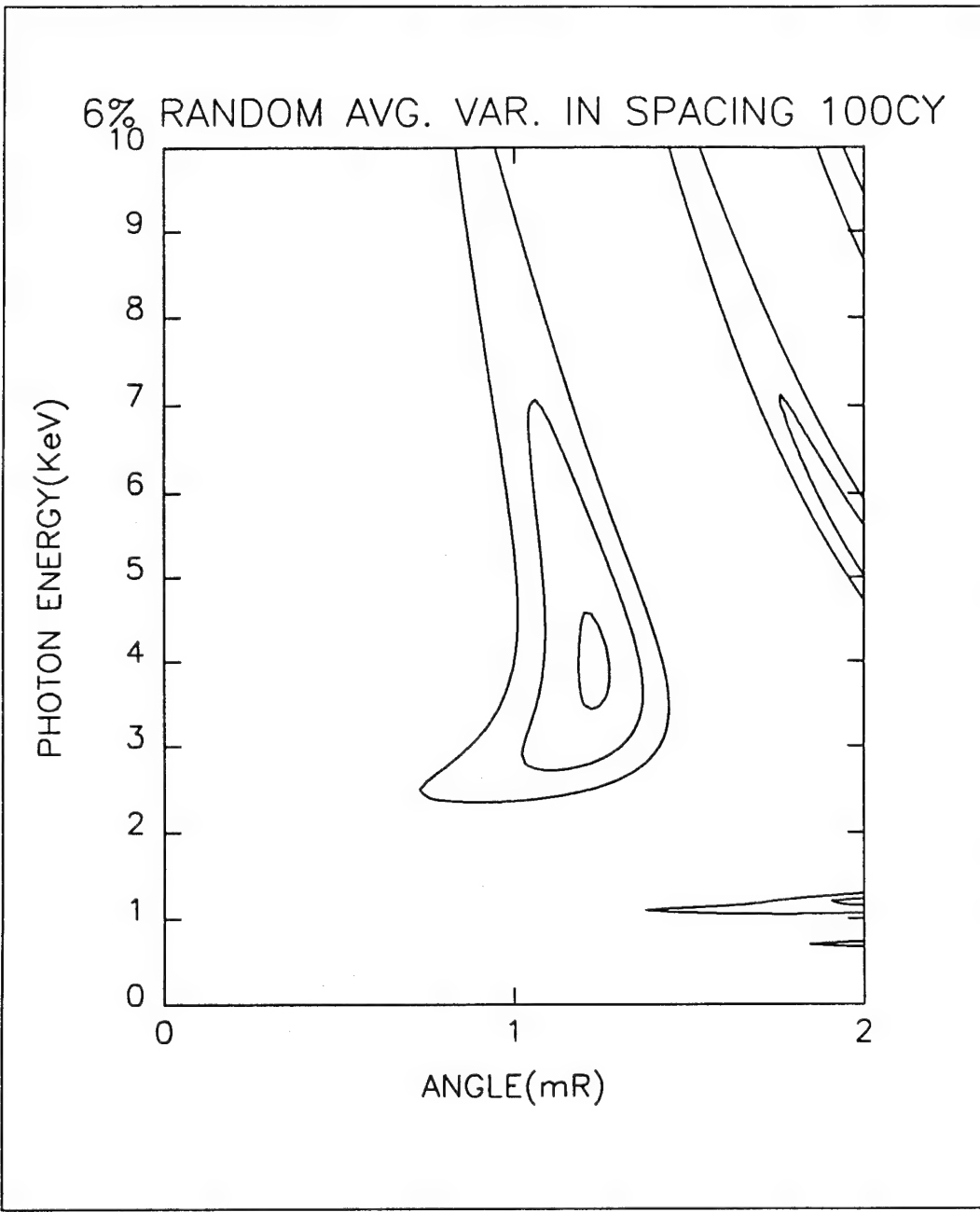


Fig. 7 Modeling the product  $F_2F_3$  with 4 Kapton foils,  $l_1 = 7.5 \mu\text{m}$ ,  $l_2 = 169 \mu\text{m}$ , for 100 cycles to calculate an average. Intensity contours match with Fig. 6. Maximum intensity = 62.829. 6% randomness in spacing.

## **V. MODELING VARIATIONS FOR A STACK OF FOUR FOILS**

In considering variations, the first case examined is random spacing. The foil thickness held fixed and precise, while the spacing is allowed to vary by a certain percent randomness. The algorithm described in the previous chapter was used with 10 cycles. The process was done for 10 percent randomness increments from 0 to 100 percent. In addition to plotting intensity contours, the value of the maximum intensity was also recorded. The intensity contours for two different degrees of randomness are shown in Fig. 8 and 9. As can be seen in the figures, the increasing randomness in spacing has the effect of narrowing the energy range of the radiation as the randomness is increased..

The second case is the opposite of the first. The spacing is held constant and the foil thickness is allowed to vary. Again, the intensity contours were computed for the same range, and the value of the maximum intensity recorded. Plots to contrast with Fig. 8 and 9 are shown in Fig. 10 and 11. This time the figures show that the increasing randomness in foil thickness has the effect of narrowing the angular spread of the radiation as the randomness is increased.

The third case is where both the foil thickness and the spacing vary by the same percent randomness. In this case the peak intensity dropped much quicker than in the first two cases. Both the energy narrowing of the spacing variations and the angular narrowing of the foil thickness variations appear to be more than just additive as randomness increases. Intensity contours for the first two values of randomness are shown in Fig. 12 and 13. Comparing the 20 percent randomness plot for the three cases, Fig. 8,10, and 13, shows the rapidity of this effect.

The value of the maximum intensity also decreases as randomness increases. Fig. 14 shows the plot of the maximum intensity for all three cases as randomness increases. The ordinate in the figure is the normalized maximum intensity, that is the calculated value divided by the maximum value for four foils. In this figure, the solid line represents randomness in spacing only, the dotted line represents randomness in foils

only, and the dashed line represents randomness in both foils and spacing. The same representation is used throughout the paper. The figure shows that the spacing variations have less of an effect in the maximum than the foil variations. Also, if one variable, either spacing or foil thickness , can be held to small random variations, the other variable can have considerable randomness and the peak will still be close to the maximum intensity of the idealized stack. This may be a more cost effective way to construct the foil stacks. For example, if both foil and spacing have 10 percent randomness, the maximum intensity will be at 87.5%. If the foils were precise, the spacing could vary by up to 25% and still be above this value.

In the idealized foils chapter, additional foils showed the effect of increasing the maximum intensity and narrowing the angular spread. The variations study described above was conducted for the same three cases for an eight foil stack. The effects of variations on the intensity of an eight foil stack became evident much quicker than for four foils as randomness increased. Not only did the maximum value drop faster, but the radiation intensity pattern also seemed to break down . In the four foil case, variations in either spacing or foils caused a narrowing in angle or energy respectively, but the radiation intensity pattern could still be seen. The intensity contours of an idealized eight foil stack are shown in Fig. 4. The deterioration of the radiation intensity pattern for eight foils is shown in Fig. 15-18. In each plot, both foil and spacing vary by the same percent randomness. As seen in Fig. 16, the radiation pattern begins to deteriorate at 20% randomness and is totally gone by 40% randomness, Fig. 18. A contrasting plot of the maximum intensity value for eight foils is shown in Fig. 19. Each of the three cases is shown, as in Fig. 14. In the eight foil case, Fig. 19 shows the maximum intensity falls about 10% faster with increasing randomness than the four foil plot in Fig. 14.

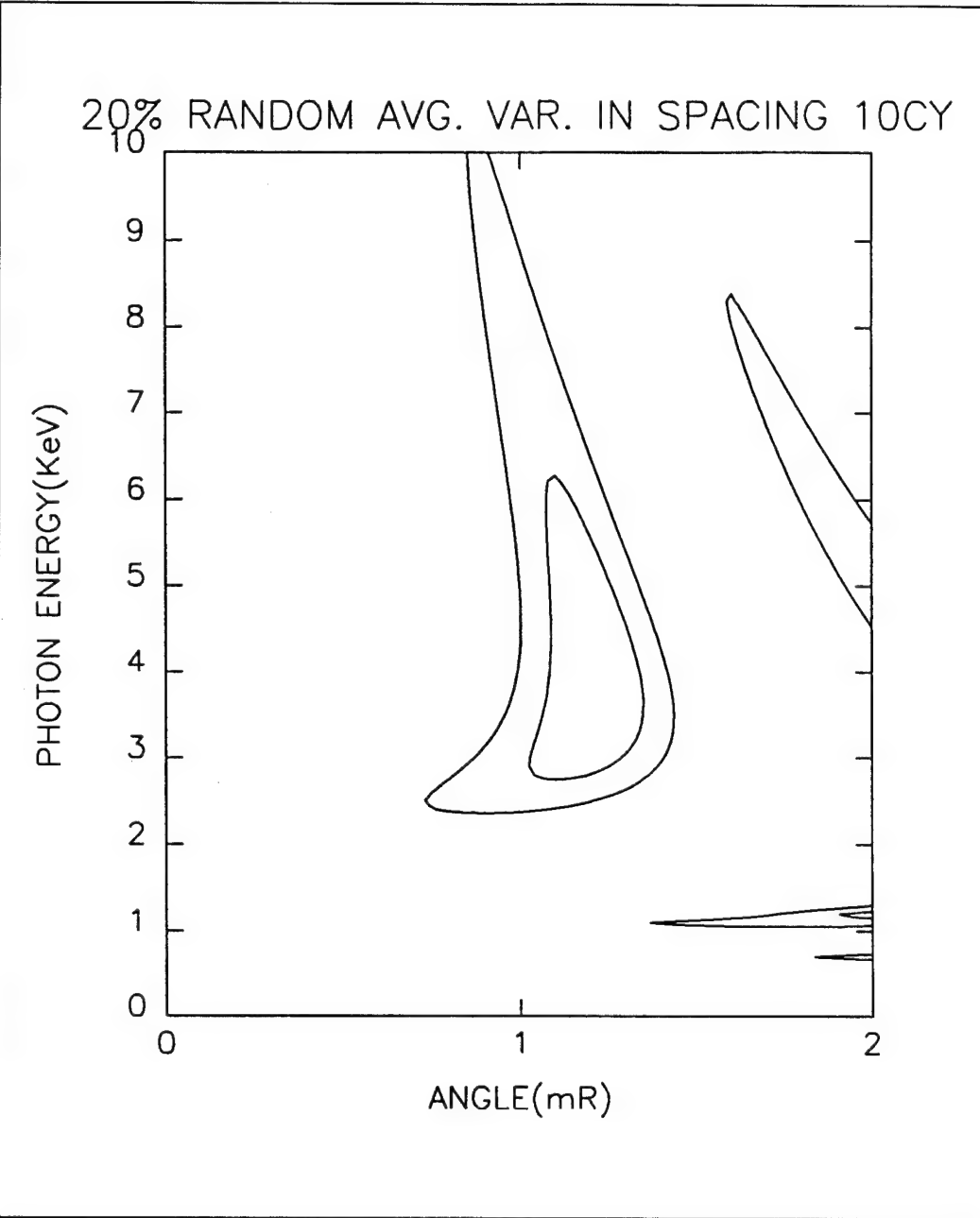


Fig. 8 20% randomness in spacing for the product  $F_2F_3$  with 4 Kapton foils,  $l_1 = 7.5 \mu\text{m}$ ,  $l_2 = 169 \mu\text{m}$ , for 10 cycles. Maximum intensity = 58.201.

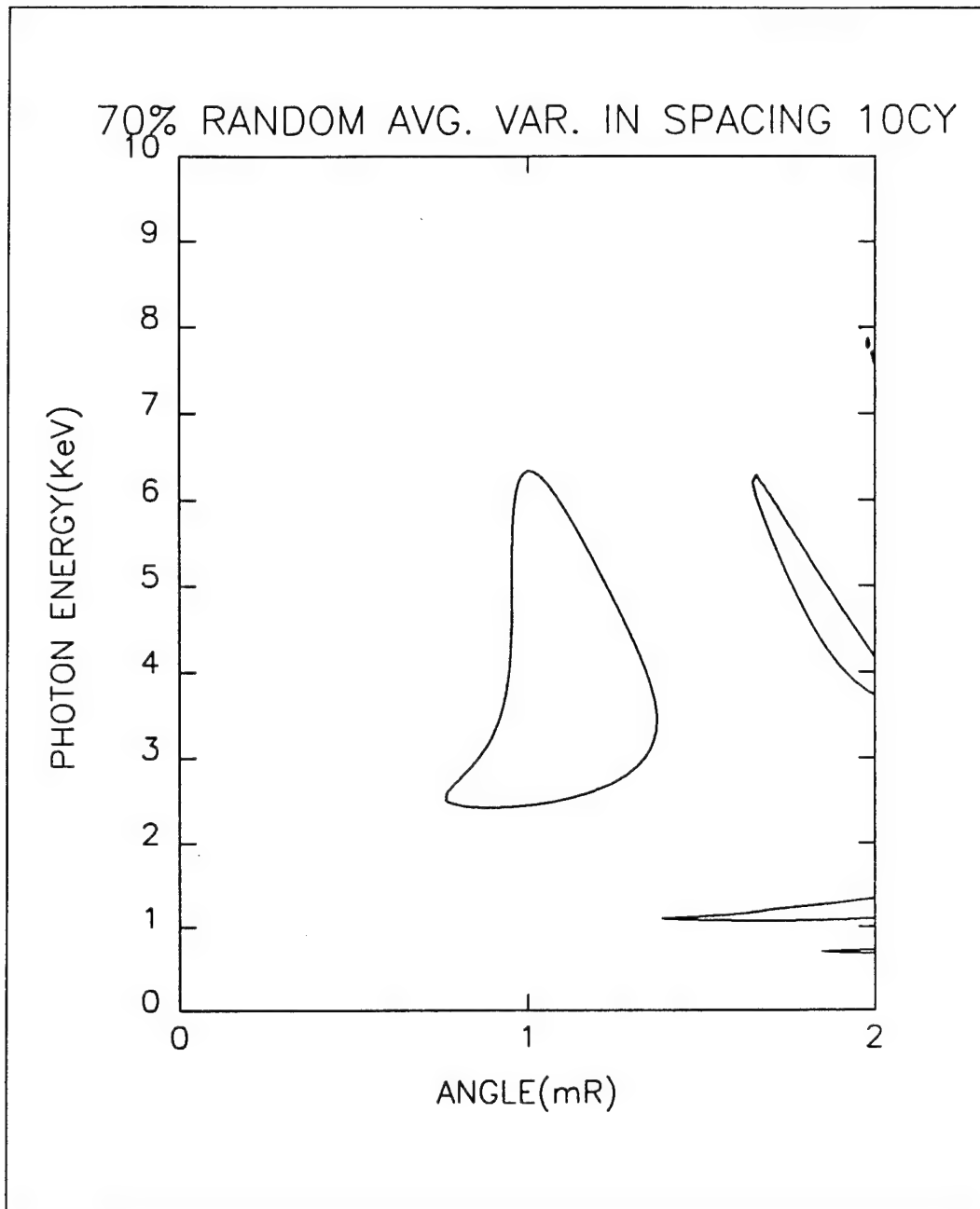


Fig. 9 70% randomness in spacing for the product  $F_2F_3$  with 4 Kapton foils,  $l_1 = 7.5 \mu\text{m}$ ,  $l_2 = 169 \mu\text{m}$ , for 10 cycles. Maximum intensity = 33.778. Note the narrowing in energy range compared to Fig. 8.

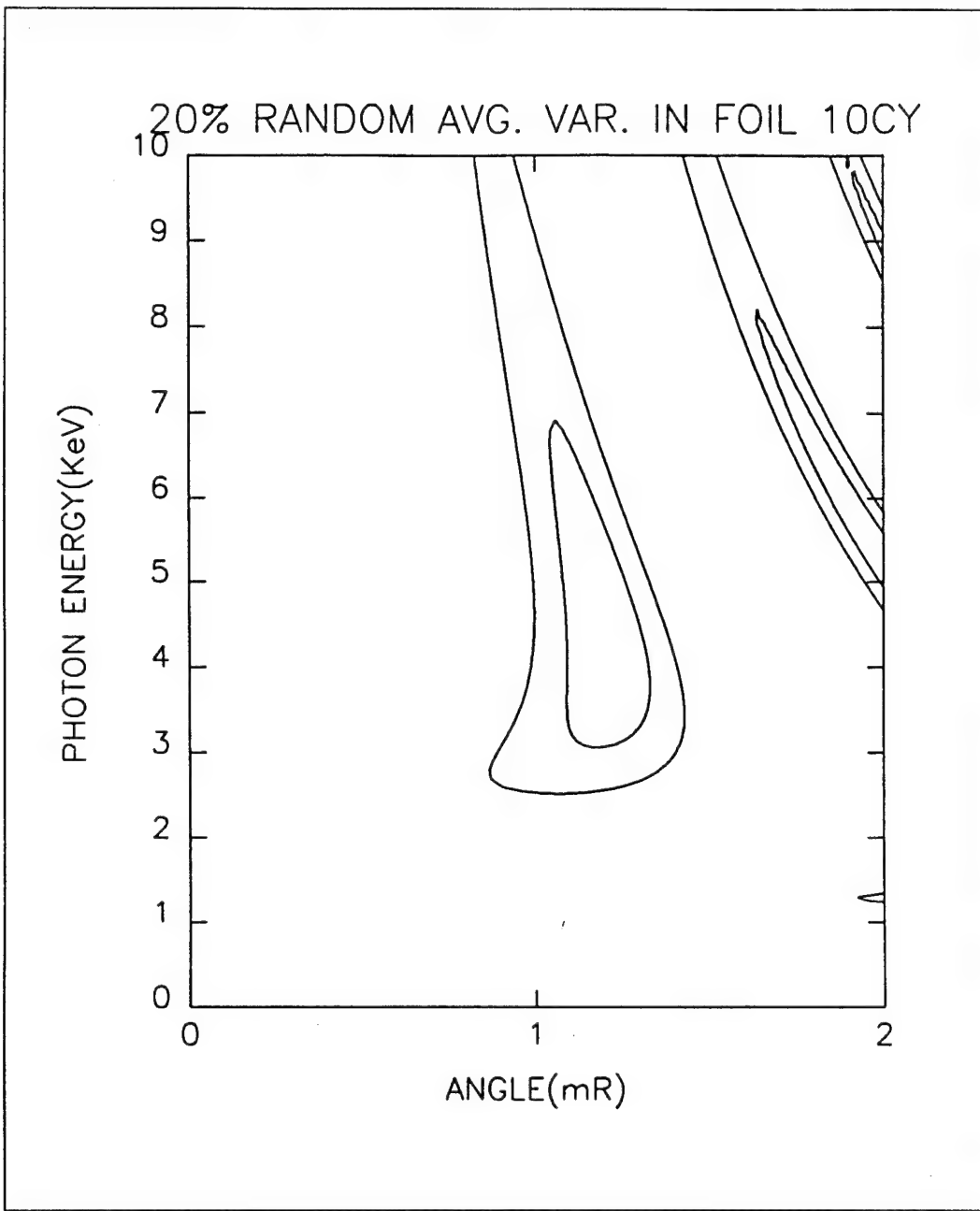


Fig. 10 20% randomness in foils for the product  $F_2F_3$  with 4 Kapton foils,  $l_1 = 7.5 \mu\text{m}$ ,  $l_2 = 169 \mu\text{m}$ , for 10 cycles. Maximum intensity = 54.240.

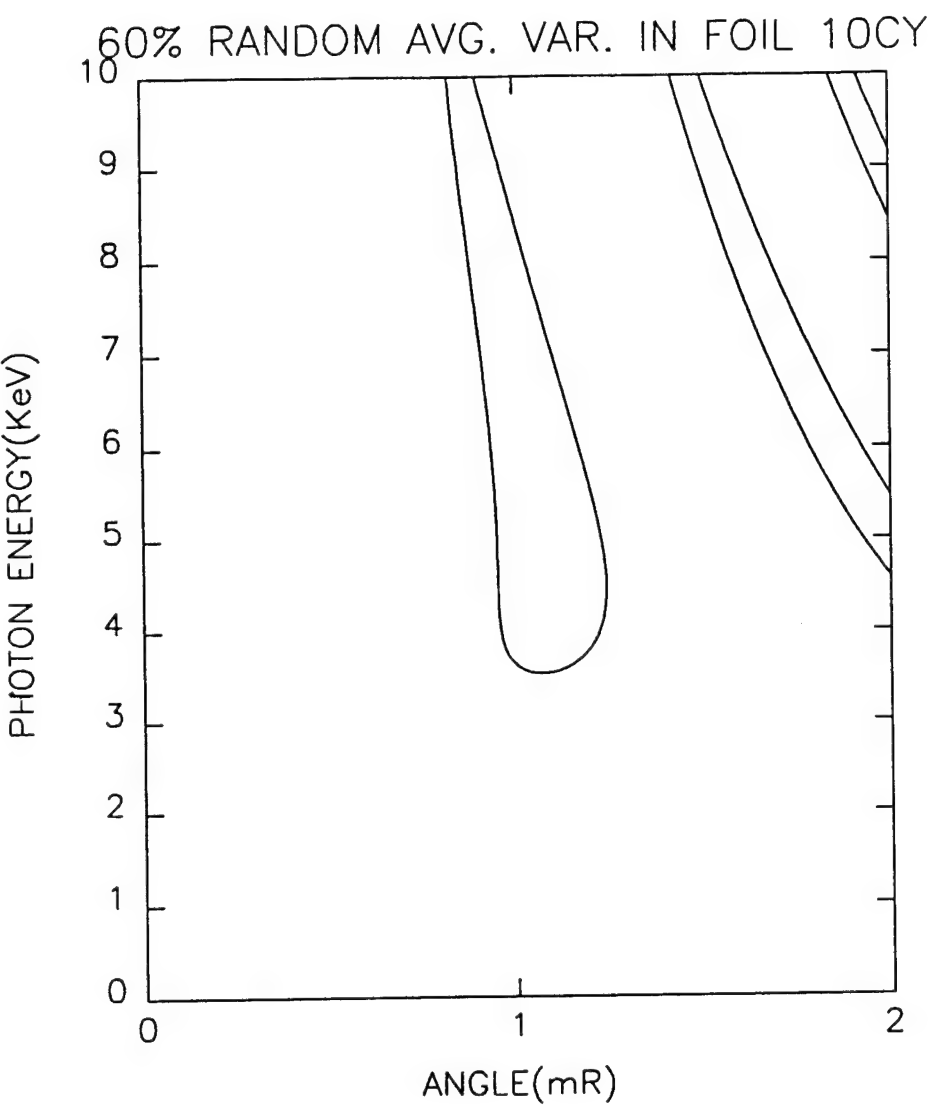


Fig. 11 70% randomness in foils for the product  $F_2F_3$  with 4 Kapton foils,  $l_1 = 7.5 \mu\text{m}$ ,  $l_2 = 169 \mu\text{m}$ , for 10 cycles. Maximum intensity = 30.602. Angular range of main maximum is much narrower than Fig. 10.

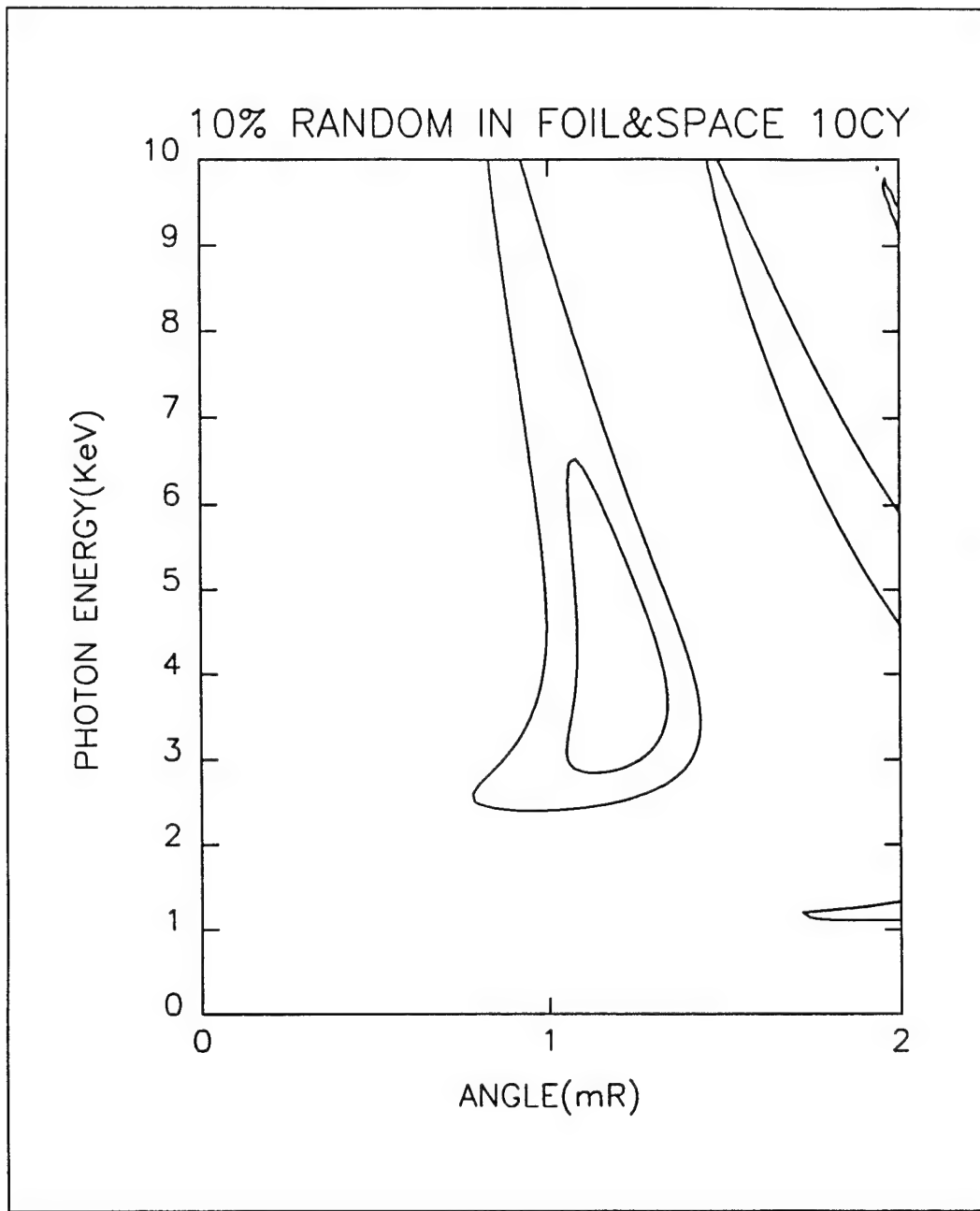


Fig. 12 10% randomness in foil and spacing for the product  $F_2F_3$  with 4 Kapton foils,  $l_1 = 7.5 \mu\text{m}$ ,  $l_2 = 169 \mu\text{m}$ , for 10 cycles. Maximum intensity = 56.261.

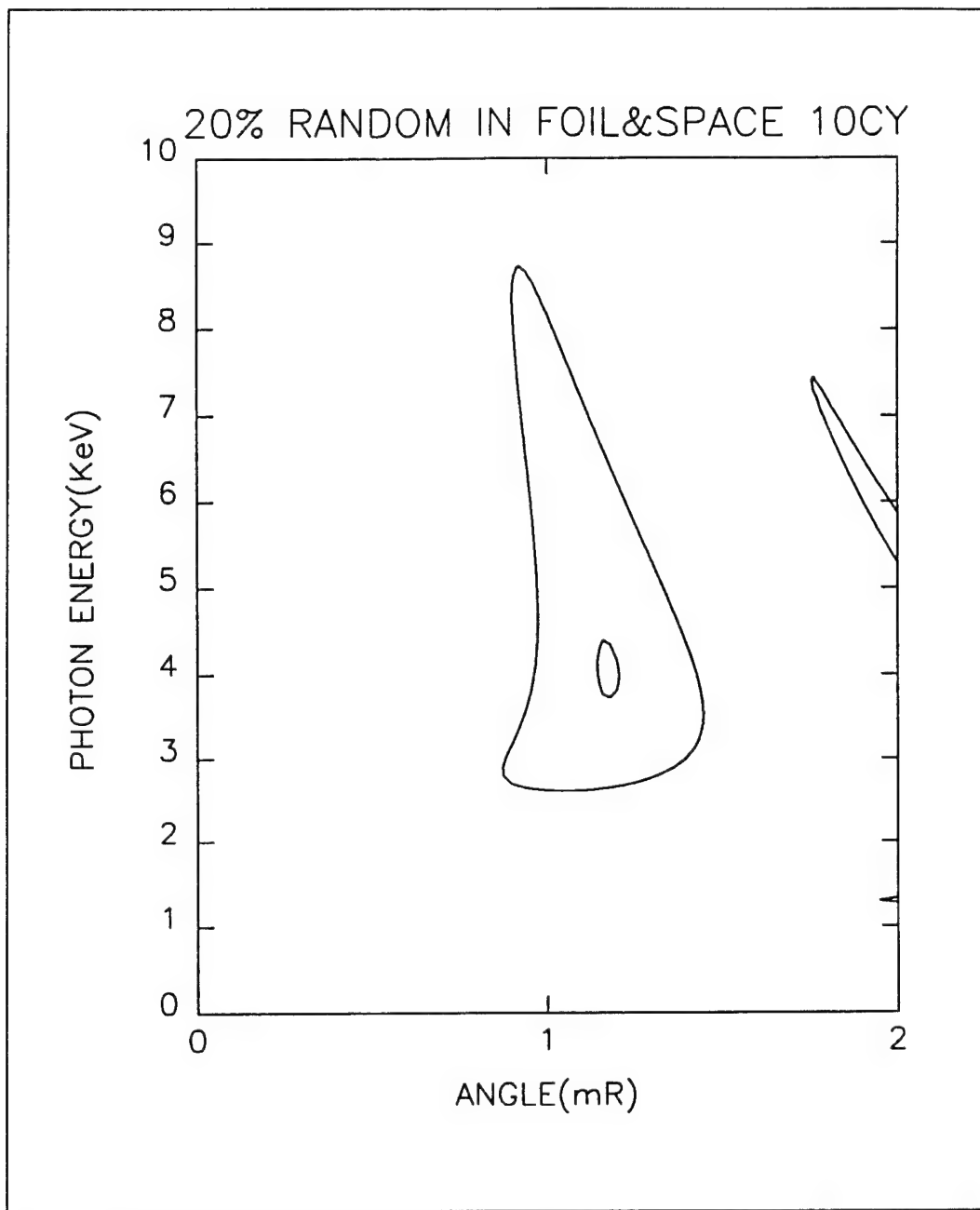


Fig. 13 20% randomness in foil and spacing for the product  $F_2F_3$  with 4 Kapton foils,  $l_1 = 7.5 \mu\text{m}$ ,  $l_2 = 169 \mu\text{m}$ , for 10 cycles. Maximum intensity = 40.593. Note decrease in energy and angular width compared to Fig. 12.

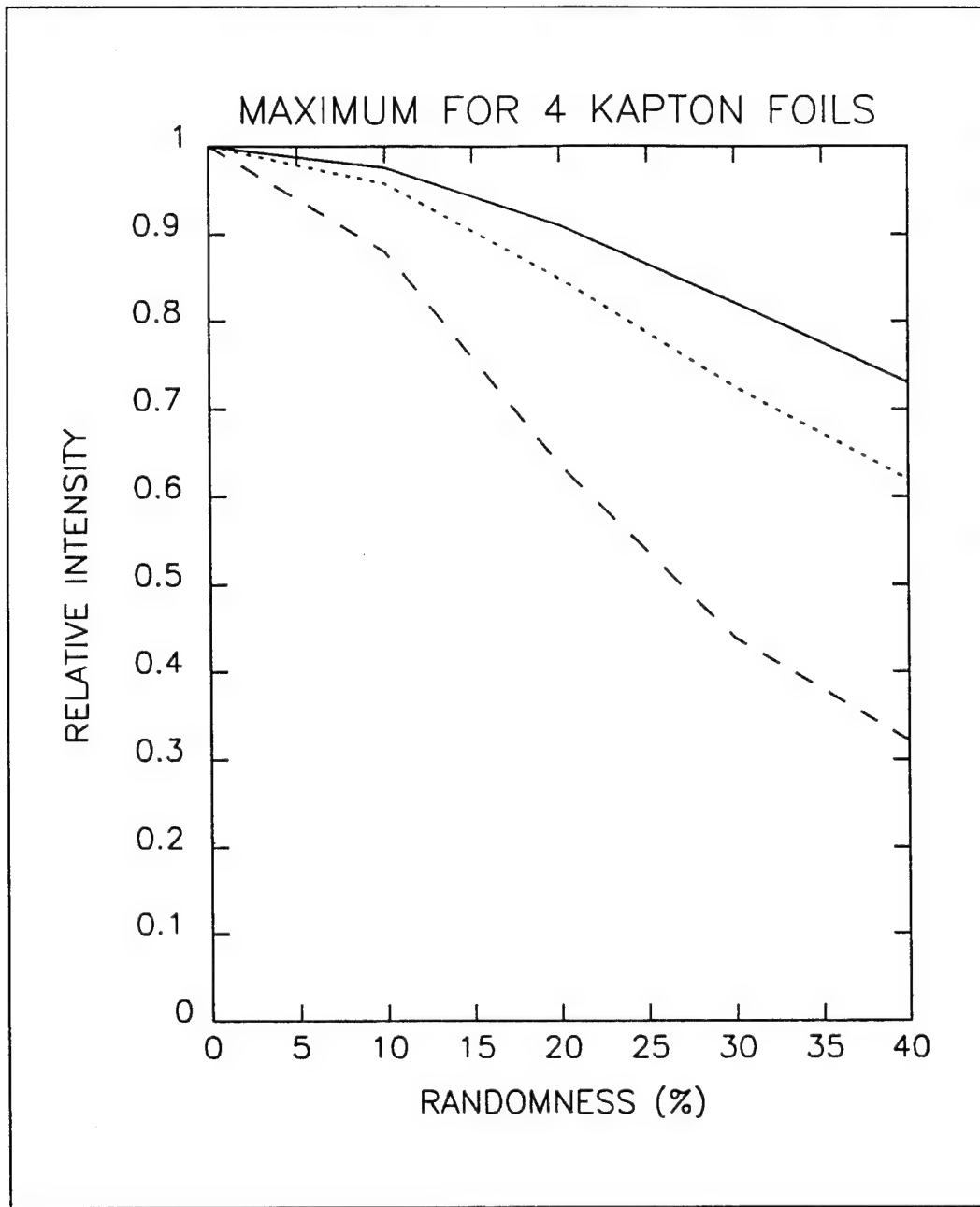


Fig. 14 Plot of maximum intensity as randomness increases for 4 Kapton foils. Solid line represents variations in spacing only. Dotted line represents variations in foils only. Dashed line represents variations in both foil and spacing.

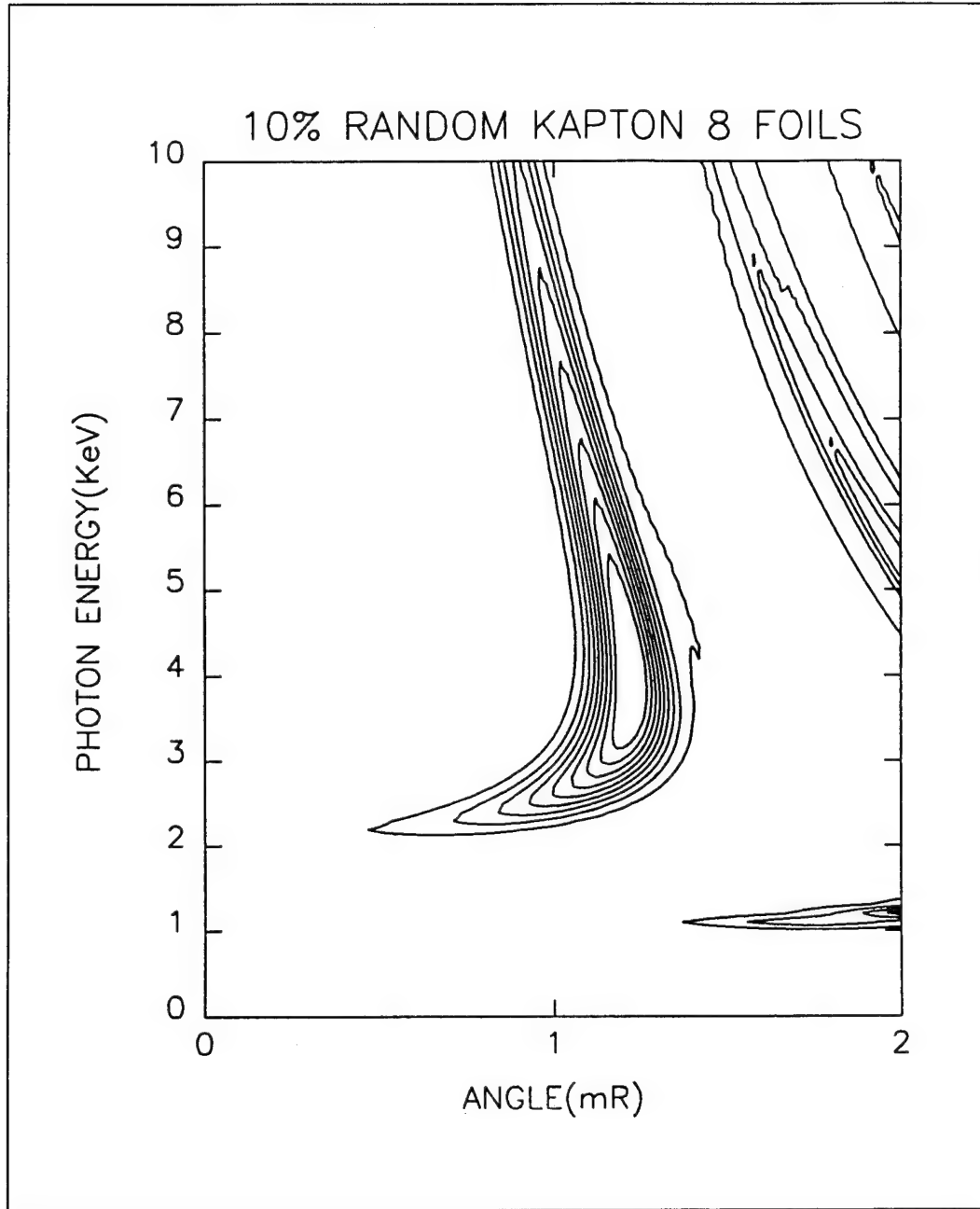


Fig. 15 10% randomness in foil and spacing for the product  $F_2F_3$  with 8 Kapton foils,  
 $l_1 = 7.5 \mu\text{m}$ ,  $l_2 = 169 \mu\text{m}$ , for 10 cycles. Radiation intensity pattern still coherent.

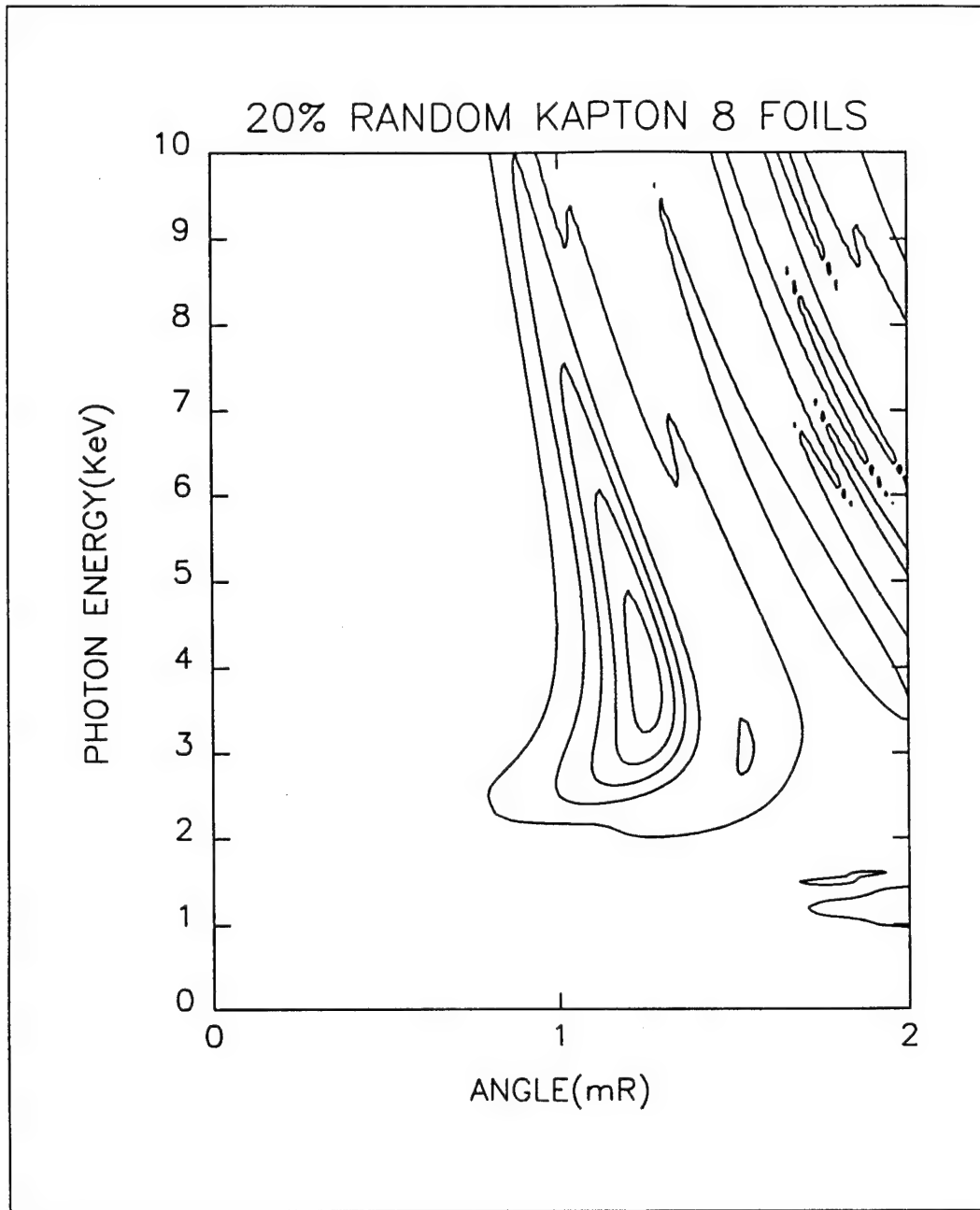


Fig. 16 20% randomness in foil and spacing for the product  $F_2F_3$  with 8 Kapton foils,  
 $L_1 = 7.5 \mu\text{m}$ ,  $L_2 = 169 \mu\text{m}$ , for 10 cycles. Note beginning of the deterioration of radiation  
intensity pattern.

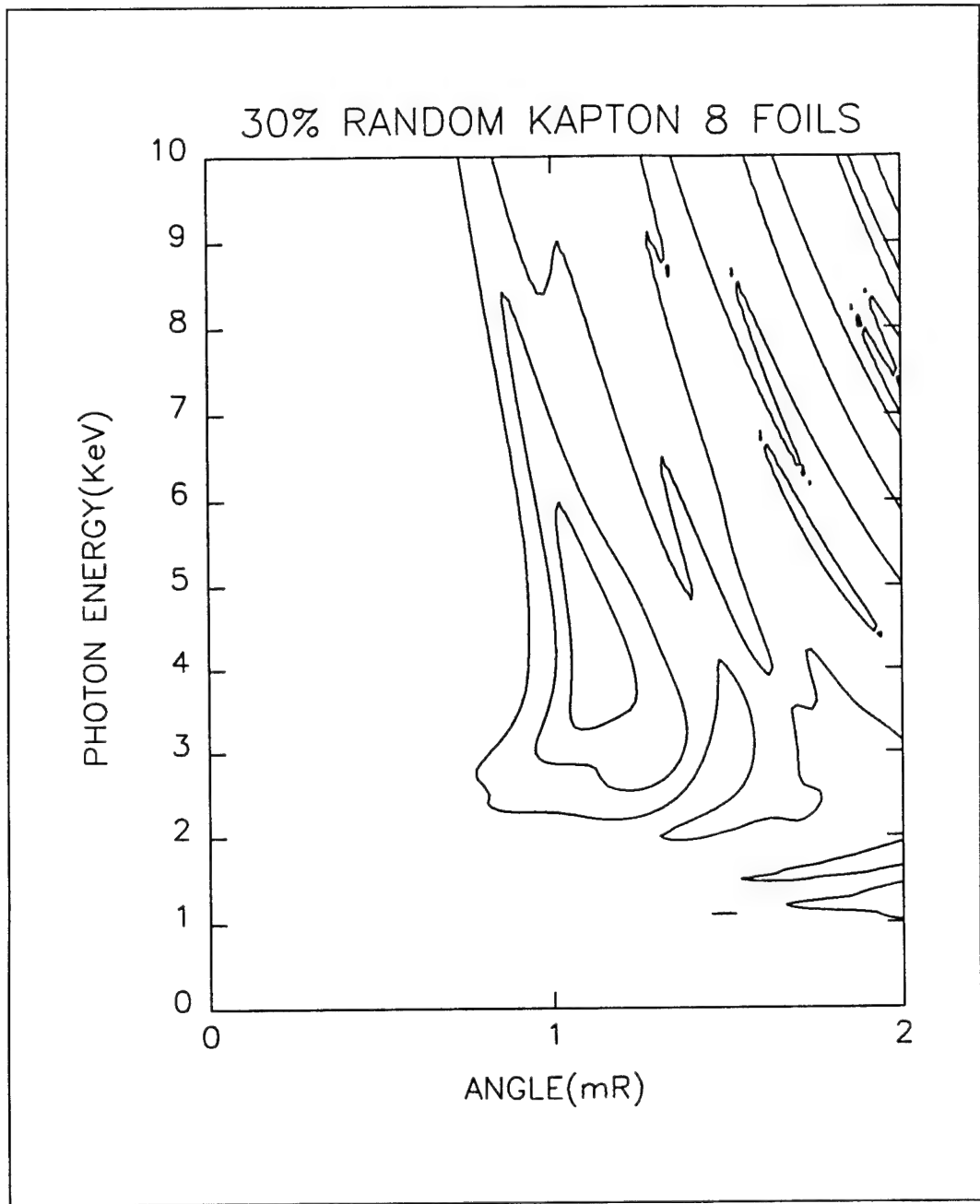


Fig. 17 30% randomness in foil and spacing for the product  $F_2F_3$  with 8 Kapton foils,  $l_1 = 7.5 \mu\text{m}$ ,  $l_2 = 169 \mu\text{m}$ , for 10 cycles. Further deterioration of radiation intensity pattern.

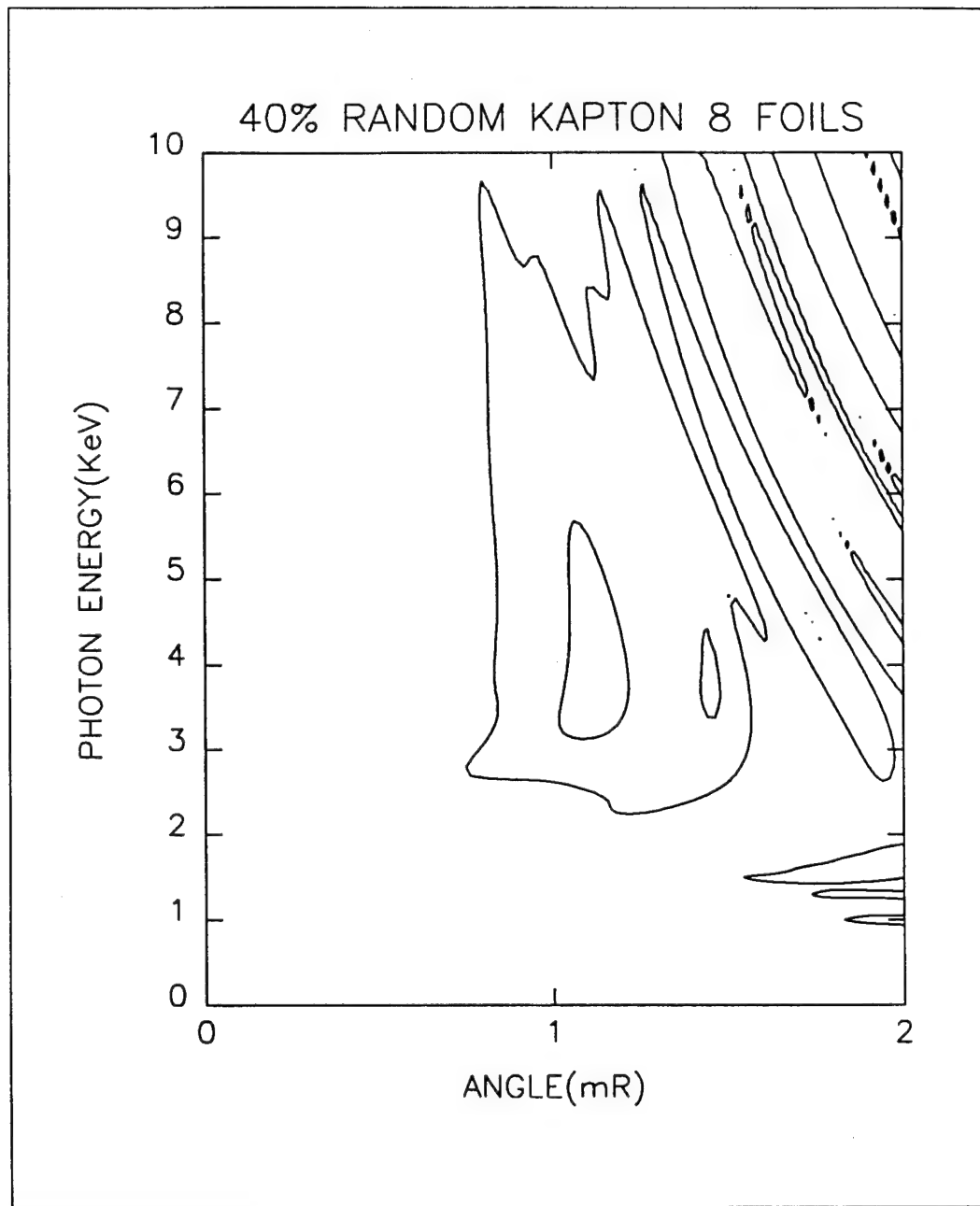


Fig. 18 40% randomness in foil and spacing for the product  $F_2 F_3$  with 8 Kapton foils,  
 $l_1 = 7.5 \mu\text{m}$ ,  $l_2 = 169 \mu\text{m}$ , for 10 cycles. Radiation intensity pattern totally deteriorated.

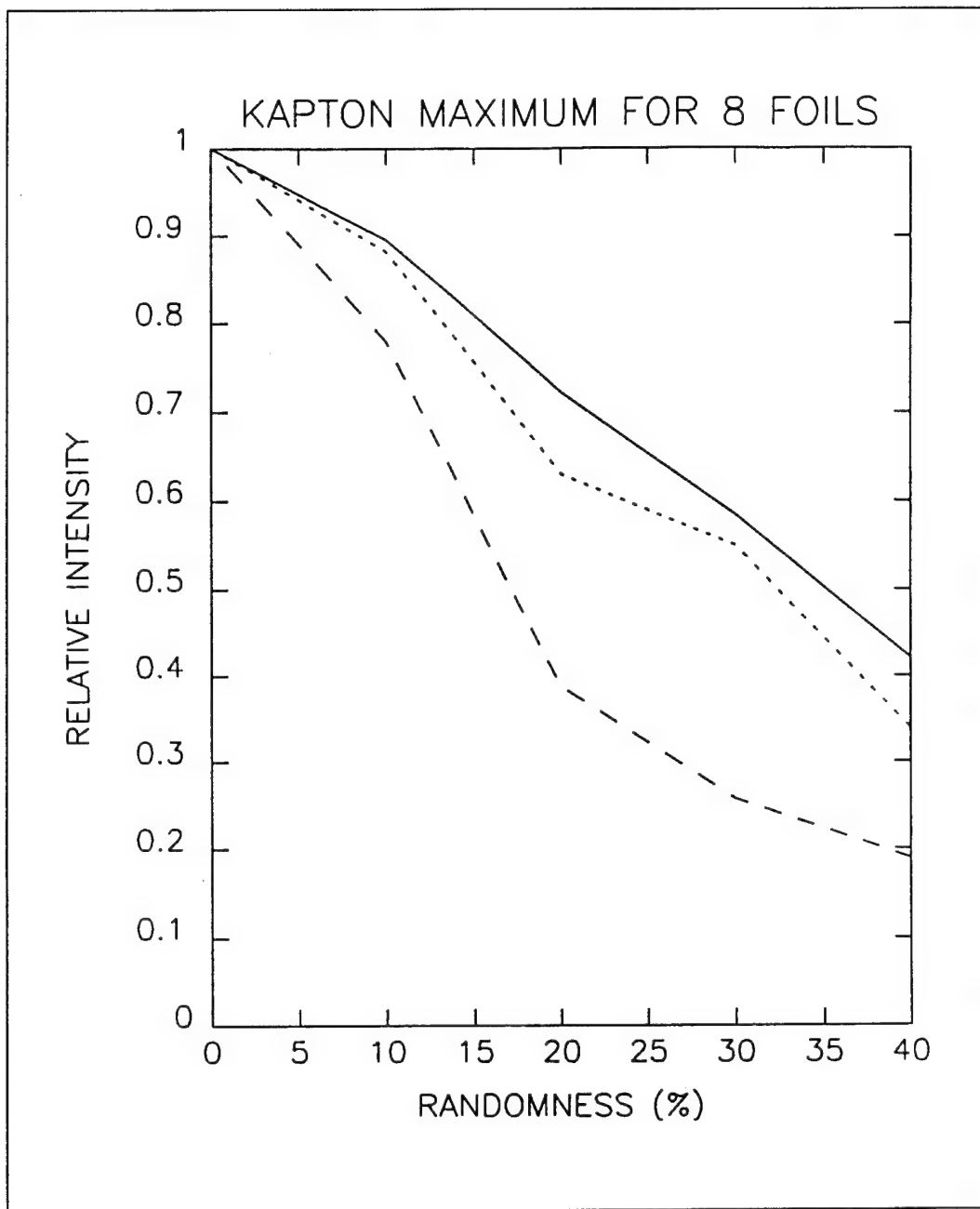


Fig. 19 Plot of maximum intensity as randomness increases for 8 Kapton foils. Solid line represents variations in spacing only. Dotted line represents variations in foils only. Dashed line represents variations in both foil and spacing. Compare to Fig. 14.

## VI. EFFECT OF ABSORPTION

In considering absorption, the same algorithm is used as in the previous section. However, the effect of the imaginary part of the permitivity which will effectively absorb part of the photons produced must be considered. To do this, a new term[Ref. 3] is added to Eq. 12,

$$A_m = -2\mu i \sum_{k=m+2}^m a_k - \varphi \sum_{k=m+2}^N a_k - \varphi_0 \sum_{k=m+2}^N b_{k-1}, \quad (17)$$

where  $\mu$  is the absorption coefficient of the material and is given by:

$$\mu = c_1 E^{c_2}, \quad (18)$$

where  $c_1$  and  $c_2$  are constants depending on the material and  $E$  is the energy.[Ref. 4]

Determining the absorption constants for different elements was done using the Nuclear Data Tables[Ref. 5]. Using the Photo A column for the element, a linear regression was done for this column versus energy with:

$$\log_{10} A = c_2 E + b$$

where  $A$  is the value of the Photo A column and  $E$  is the energy in keV. From the regression, the value of  $c_2$  for Eq. 18 is obtained directly. The value of  $c_1$  is

$$c_1 = m 10^b$$

where  $m$  is the atomic concentration.[Ref. 4]

The absorption coefficients were determined for three materials, Kapton, Aluminum, and Titanium. For the case where the foils are made of Kapton, with the same dimensions as Fig. 3, the result for absorption taken into account is plotted in Fig. 20 with no random variations. The figure shows what Eq. 17 predicts, since  $c_2$  is negative, the effects of absorption are greatest for low energy. In Fig. 20, the radiation intensity is attenuated strongly below 2.5 keV and less above that value. The maximum intensity value, as expected, is slightly lower as compared to Fig. 6 with value of 61.156. This figure shows the effects of absorption in Kapton is rather small with no variations.

The case of absorption in Aluminum with no random variations is plotted in

Fig. 21. Since the value of  $c_1$  is a factor of ten higher for aluminum than Kapton, the absorption is much higher and the radiation below 4 keV is attenuated. The value of the maximum intensity is 44.626, much lower than Kapton. Aluminum has a K edge at 1.5 keV, so the values of  $c_1$  and  $c_2$  remained constant over the range of energy in this calculation.

The case of absorption in Titanium with no variations in foil thickness or spacing, Fig. 22, shows an interesting effect. The K edge for titanium is just below 5 keV. Below the K edge, the value for  $c_1$  is on the order of aluminum, but is an order of magnitude higher above the K edge. The value for  $c_2$  remains almost the same above and below the K edge. This change in absorption at 5 keV causes the break in the radiation intensity seen in Fig. 22. The value of the maximum intensity occurs below the K edge with a value of 44.621, which, as expected, is close to aluminum.

Considering the effects of variations and absorption raised an interesting result in aluminum and titanium. As with variations in four foils, results for three cases were calculated. The three cases are randomness in spacing, randomness in foil thickness, and equal randomness in both. The above cases were averaged over 10 cycles for a particular percent randomness twice. Both values of the maximum intensity were recorded and averaged. For some values, the two values coincided well and in other cases there was considerable scatter, up to 15% of the average value.

The results of the maximum intensities calculated are plotted in Fig. 23,24, and 25 for aluminum, titanium and kapton respectively. Fig. 23 shows the results of randomness in spacing and randomness in both to give similar results for aluminum. Randomness in foil thickness had a minor effect in decreasing the maximum. This is totally different than the case of no absorption. In that case, randomness in spacing had the least effect, and randomness in both had a much greater effect than the other two cases. This plot predicts that for maximum intensity in aluminum, a stack could be made with precise spacing, and the foil thickness can vary by a wide amount. Titanium also shows this effect, Fig. 24, but not as strongly as aluminum. The plot of variations in

spacing shows several peaks in the curve for titanium compared to plot for aluminum.

These peaks are the result of the statistical averaging done in the modeling. The expected values would have a smoother curve, like the plot for aluminum.

Since absorption in kapton has little effect, in Fig. 25 the results for the three cases are similar to that of variations only, where variations in both foil and spacing have a much greater effect than the other two cases of variations in either foil or spacing.

Despite the greater absorption in titanium, the effect of the K edge can be useful. The absorption and variations can be used to make a pattern that, while lower in intensity, only occurs for a narrow energy and angle. Fig. 26 shows the effect of 20% randomness in both foil and spacing. Only the pattern below the K edge remains, the rest is absorbed. For increased intensity, eight foils with 20% randomness are plotted in Fig. 27. Since each contour represents an interval of 20, the intensity in the lowest peak is almost twice as high as the other peaks, and the energy and angular range are about the same as Fig. 26.

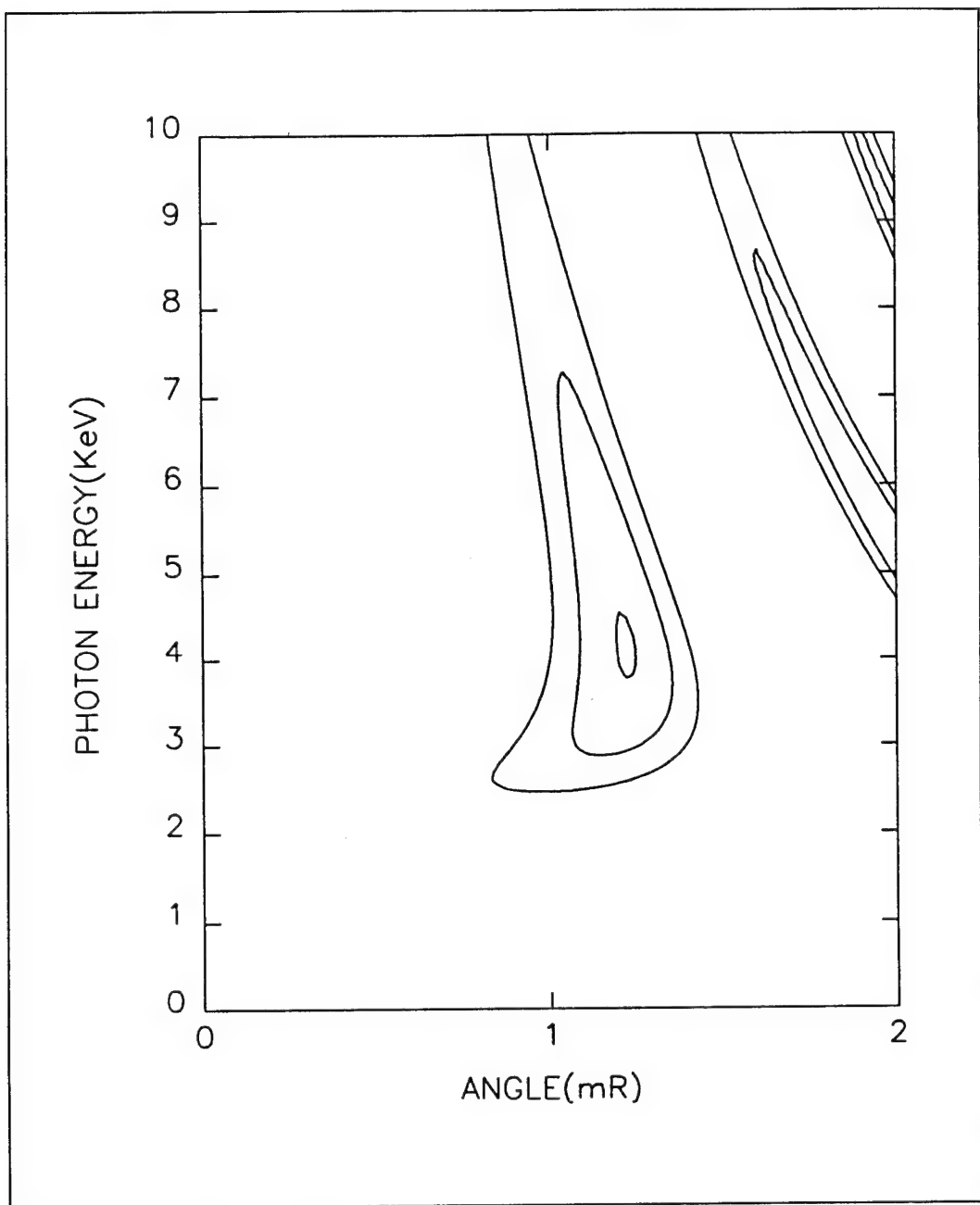


Fig. 20 No randomness in foil and spacing for the product  $F_2F_3$  with 4 Kapton foils,  
 $I_1 = 7.5 \mu\text{m}$ ,  $I_2 = 169 \mu\text{m}$ , for 10 cycles with absorption taken into account. Maximum  
intensity = 61.156.

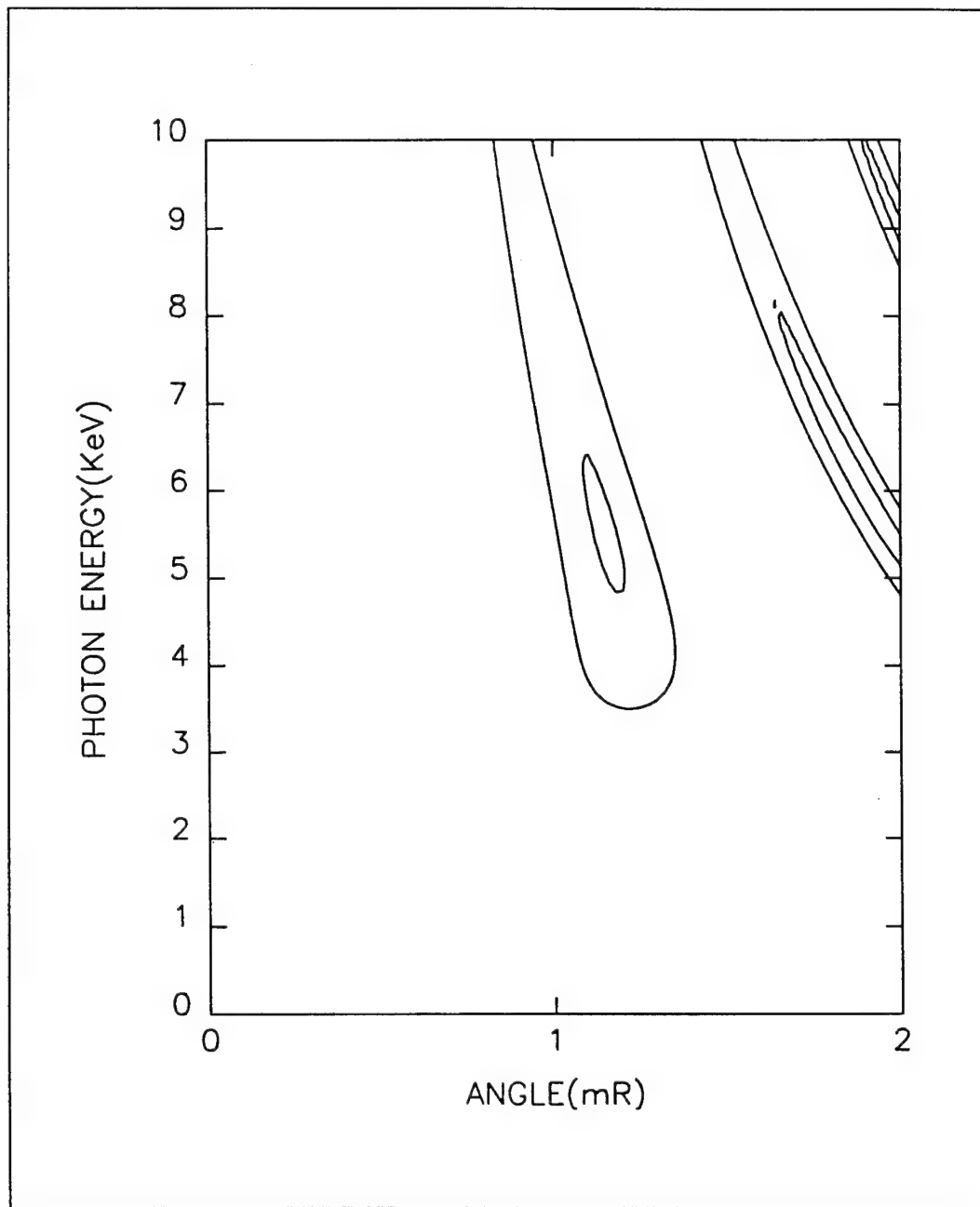


Fig. 21 No randomness in foil and spacing for the product  $F_2F_3$  with 4 Aluminum foils,  $l_1 = 7.5 \mu\text{m}$ ,  $l_2 = 169 \mu\text{m}$ , for 10 cycles with absorption taken into account. Maximum intensity = 45.626.

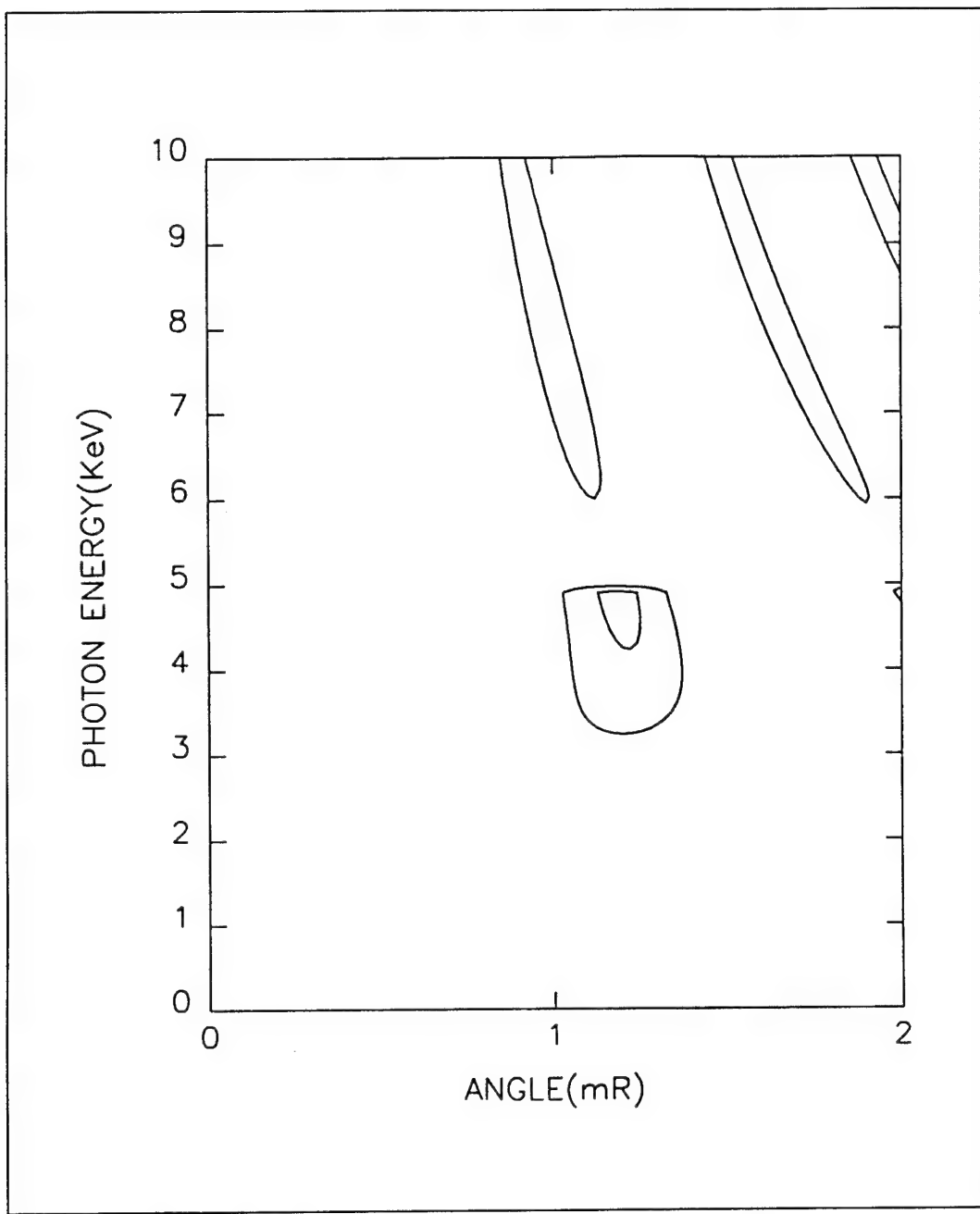


Fig. 22 No randomness in foil and spacing for the product  $F_2F_3$  with 4 Titanium foils,  
 $l_1 = 7.5 \mu\text{m}$ ,  $l_2 = 169 \mu\text{m}$ , for 10 cycles with absorption taken into account. Maximum  
intensity = 44.621.

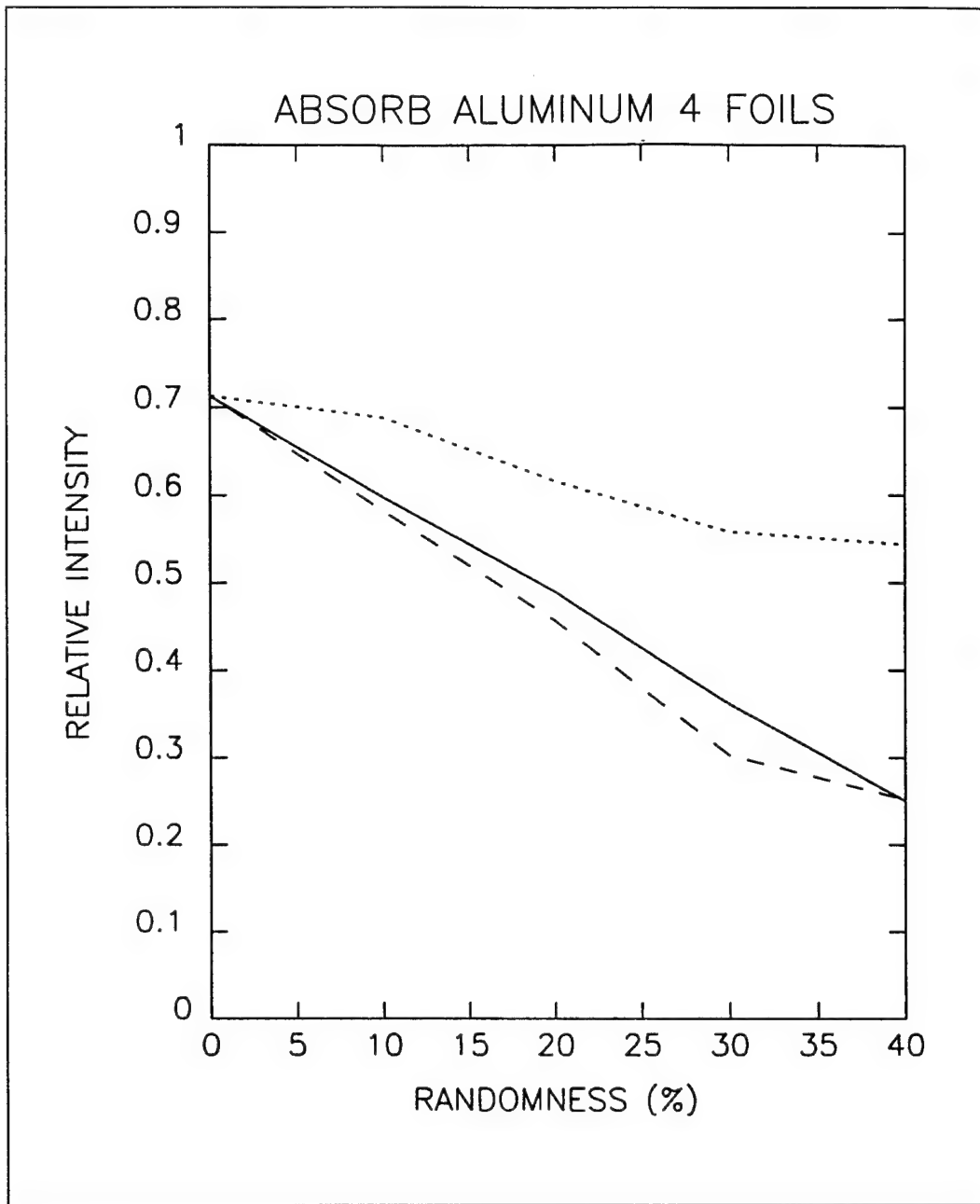


Fig. 23 Plot of maximum intensity as randomness increases for 4 Aluminum foils with absorption. Solid line represents variations in spacing only. Dotted line represents variations in foils only. Dashed line represents variations in both foil and spacing.

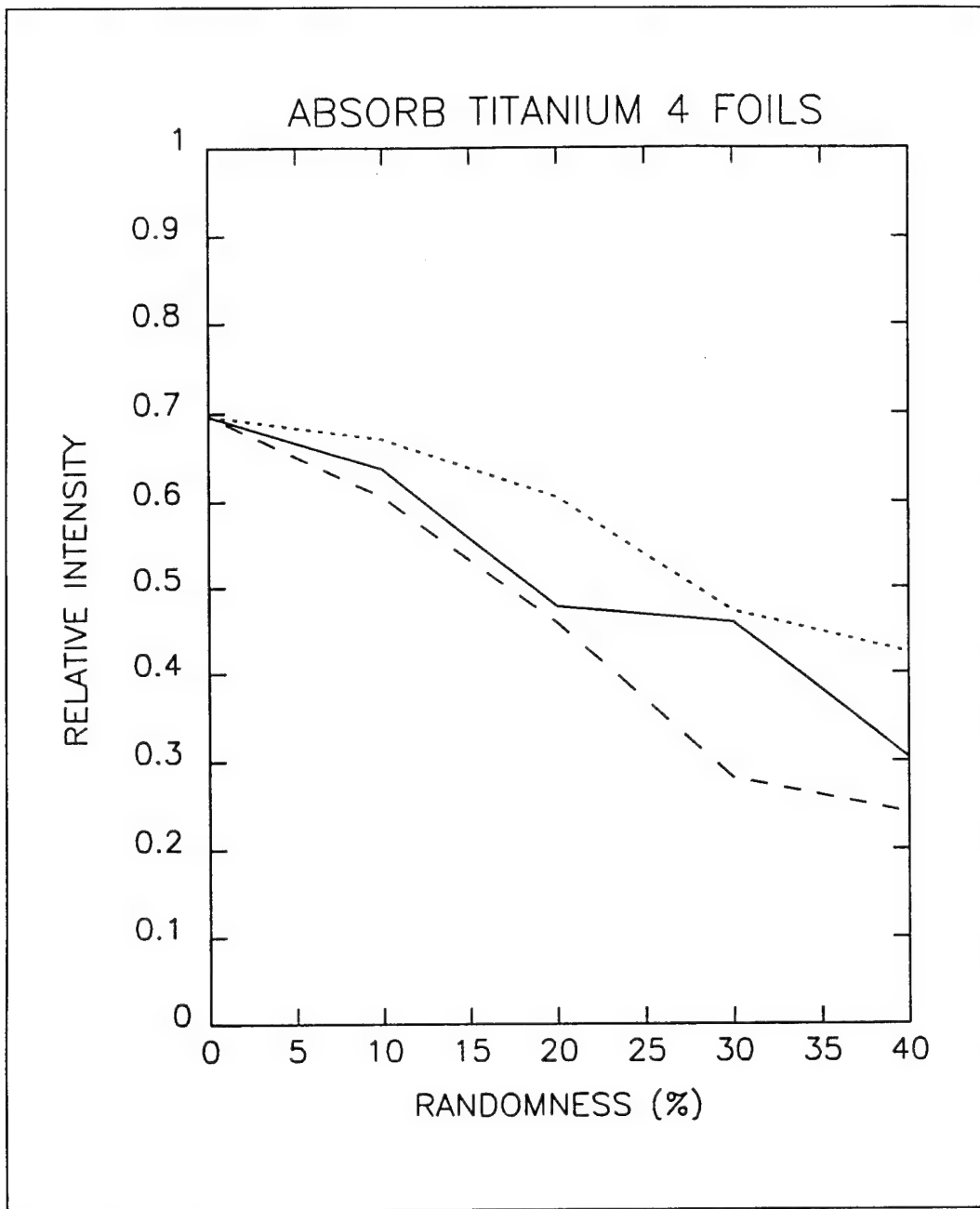


Fig. 24 Plot of maximum intensity as randomness increases for 4 Titanium foils with absorption. Solid line represents variations in spacing only. Dotted line represents variations in foils only. Dashed line represents variations in both foil and spacing.

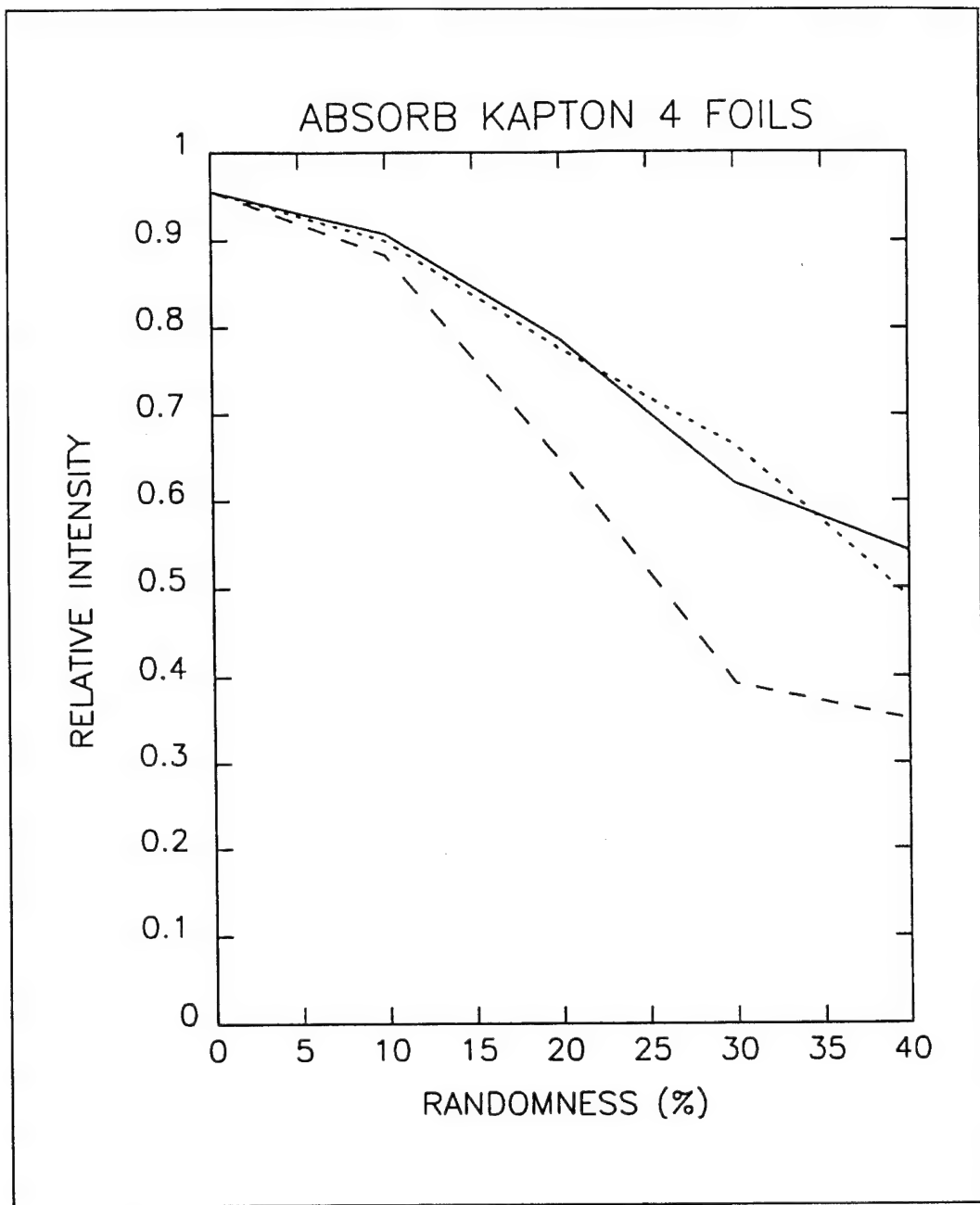


Fig. 25 Plot of maximum intensity as randomness increases for 4 Kapton foils with absorption. Solid line represents variations in spacing only. Dotted line represents variations in foils only. Dashed line represents variations in both foil and spacing.

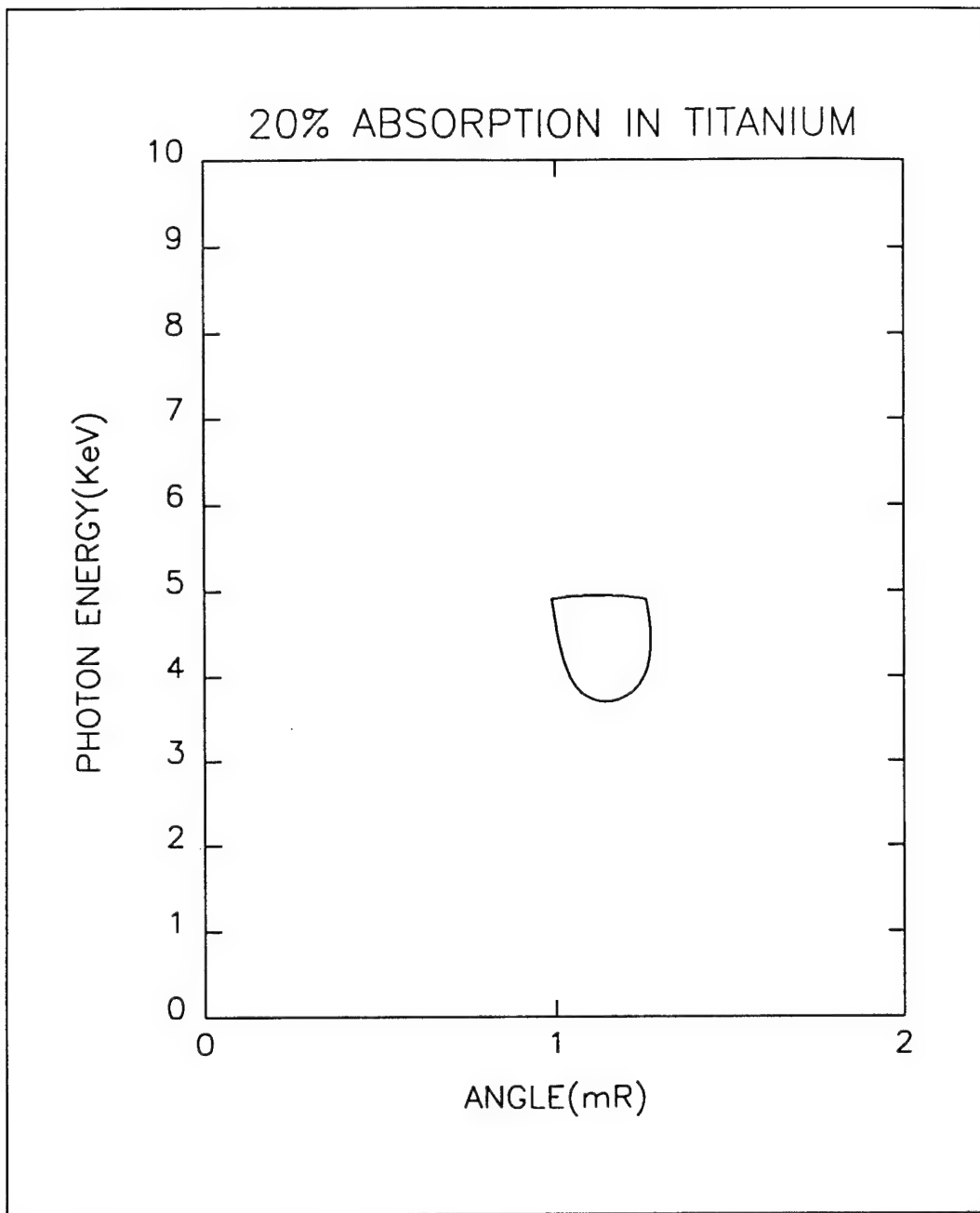


Fig. 26 20% randomness in foil and spacing for the product  $F_2F_3$  with 4 Titanium foils,  $l_1 = 7.5 \mu\text{m}$ ,  $l_2 = 169 \mu\text{m}$ , for 10 cycles with absorption taken into account. Maximum intensity = 26.758.

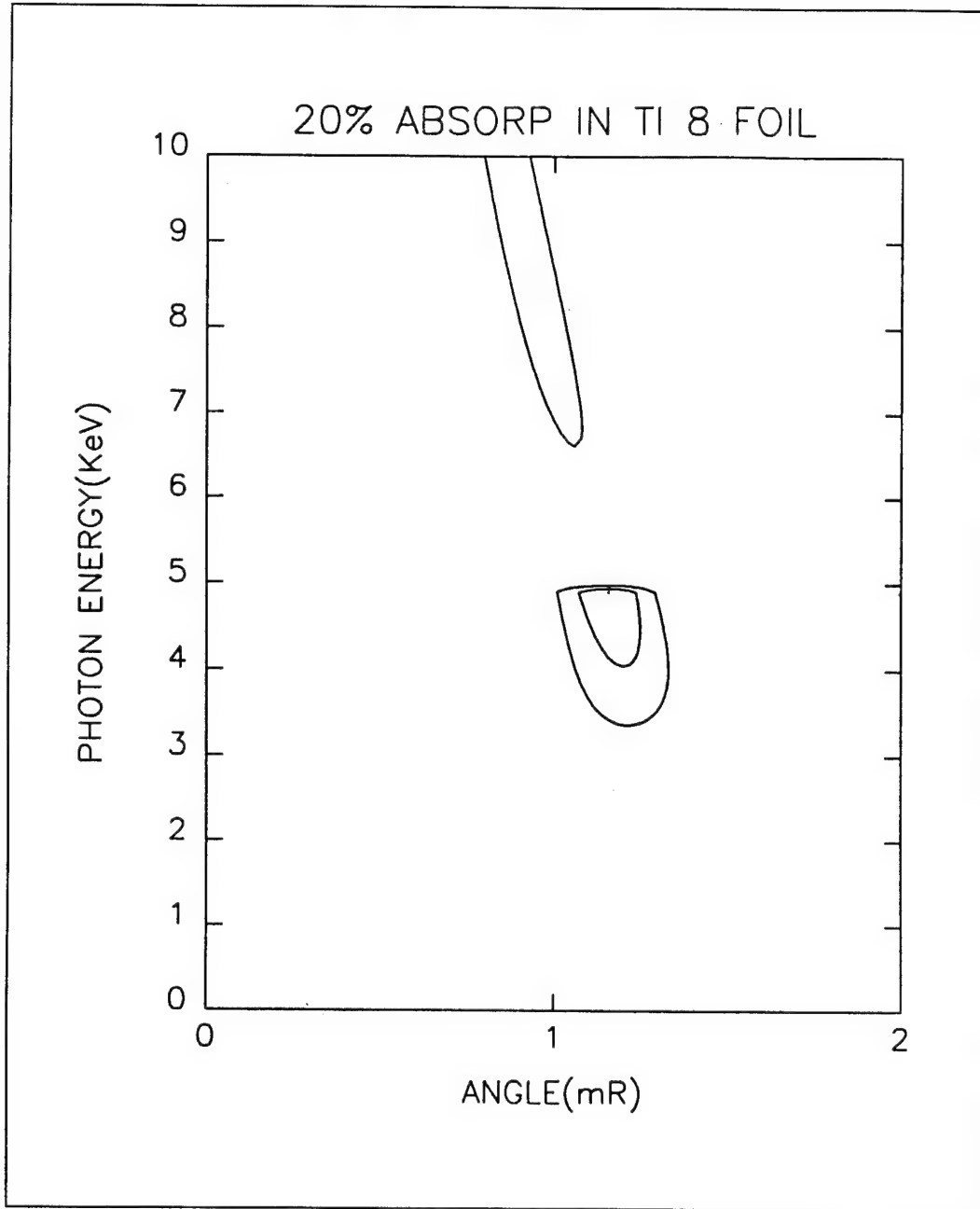


Fig. 27 20% randomness in foil and spacing for the product  $F_2F_3$  with 8 Titanium foils,  
 $l_1 = 7.5 \mu\text{m}$ ,  $l_2 = 169 \mu\text{m}$ , for 10 cycles with absorption taken into account. Maximum  
intensity = 60.084.



## VII. SELECTION OF PARAMETERS WHICH PLACE INTENSITY PEAK AT A DESIRED ENERGY AND ANGLE

Since the intensity peaks occur for particular values of energy and angle, it is interesting to examine how these two values vary as a function of  $l_1$  and  $l_2$ . Because various detectors have different capabilities, it is important to design the stack of foils to have a maximum intensity at the sensors maximum sensitivity. In order to produce a maximum, the following equations must be satisfied,

$$s = \frac{l_1 E}{hc} \left[ \frac{1}{r^2} + \theta^2 + \frac{E_p^2}{E^2} \right],$$

and,

$$r = \frac{l_1 E}{2hc} \left[ \frac{1}{r^2} + \theta^2 + \frac{E_p^2}{E^2} \right] + \frac{l_2 E}{2hc} \left[ \frac{1}{r^2} + \theta^2 \right],$$

which result from maximizing Eq. 5 and Eq. 8. This gives two equations and six unknowns which cannot be solved analytically but may be plotted for specific cases.

Consider a pattern which is produced from  $F_2 F_3$  for the particular case of the  $r=2$ ,  $s=3$  intersection with the values of  $l_1=13.5 \mu\text{m}$  and  $l_2=10.25 \mu\text{m}$  as shown in Fig. 28. As noted earlier, the maximum of  $F_1$  occurs at  $1/\gamma$ . To maximize the intensity, the  $r=2$ ,  $s=3$  intersection must be moved to this particular angle. This is accomplished by changing  $l_1$  and  $l_2$ . Fig. 29 shows the effect of changing  $l_1$  on the  $r=2$ ,  $s=3$  intersection. Increasing  $l_1$  has the effect of decreasing the angle for the intersection but increasing the energy. Increasing  $l_2$  has little effect on the angle, but decreases the energy coordinate for the intersection. To move the intersection to an angle of 0.6 mrad and energy of 4 keV, the computer calculations show that  $l_1=23.5 \mu\text{m}$  and  $l_2=450 \mu\text{m}$  is appropriate. The corresponding  $r=2$ ,  $s=3$  plot is shown in Fig. 30. The respective contour plots for

Fig. 28 and 30 are shown in Fig 31 and 32 for four Kapton foils with no absorption. The maximum for the  $r=2$ ,  $s=3$  intersection appears where predicted. Any values of  $r$  and  $s$  can be predicted in a similar manner.

One consideration in moving to thicker foils is the effect of absorption on thicker foils. For the case  $l_1=23.5 \mu\text{m}$  and  $l_2=450 \mu\text{m}$ , the absorption in four foils of kapton is shown if Fig 33. In this figure, 11% of the maximum intensity is absorbed compared to 5% in Fig. 20. As expected, the absorption is higher in thicker foils.

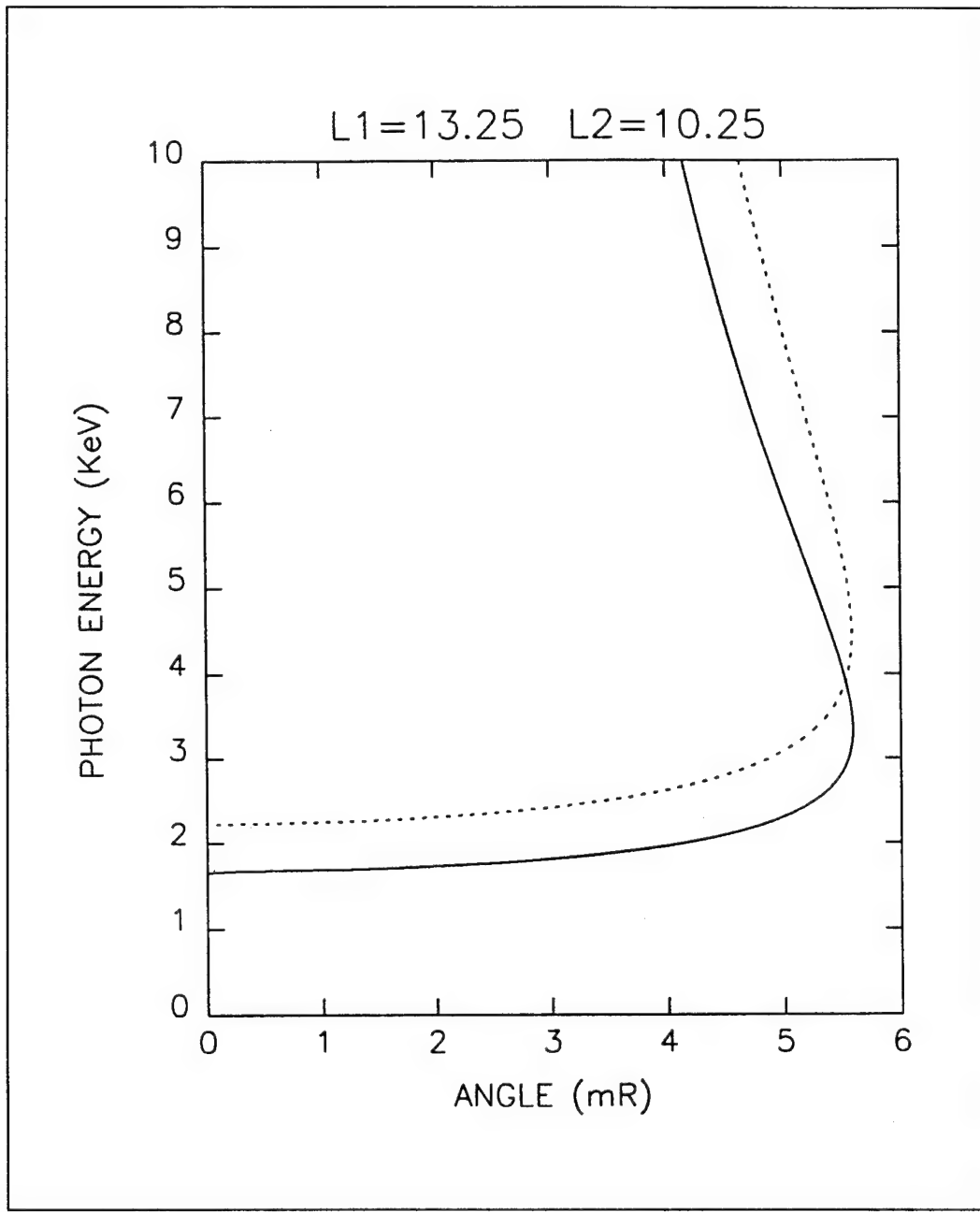


Fig. 28 With  $l_1 = 13.25 \mu\text{m}$ . 4 Kapton foils separated by a vacuum spacing of  $l_2 = 10.25 \mu\text{m}$ , the  $r=2$  maximum of  $F_2$  is represented by the dashed line. The  $s=3$  maximum of  $F_3$  is represented by the solid line. Intersections maximize the product  $F_2 F_3$ .

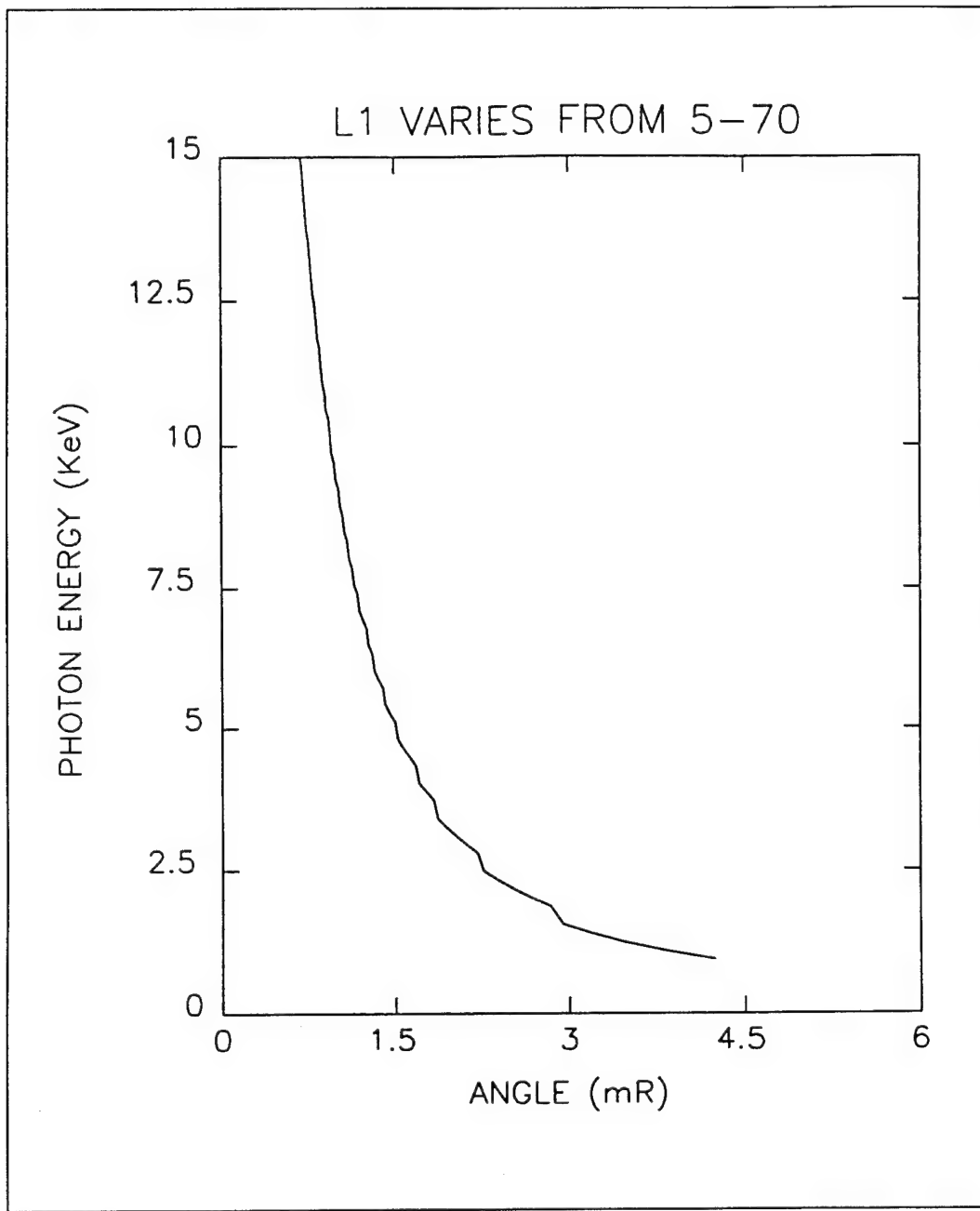


Fig. 29 Plot of the intersection of the  $r=2$ ,  $s=3$  maximum as  $l_1$  varies. Intersection moves from right to left as  $l_1$  increases, and from low energy to high energy.

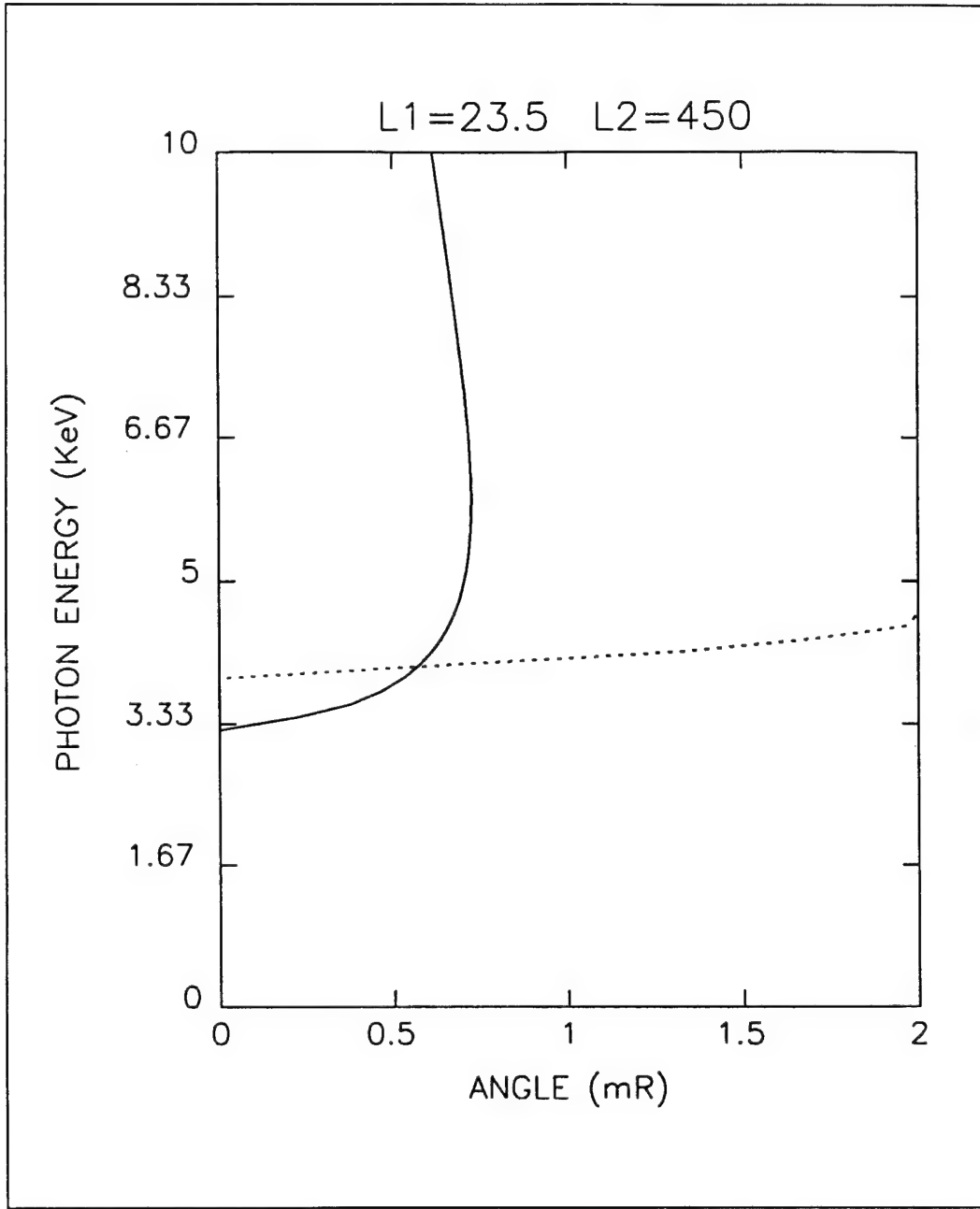


Fig. 30 With  $l_1 = 23.5 \mu\text{m}$ ,  $l_2 = 450 \mu\text{m}$ , for 4 Kapton foils, the  $r=2$  maximum of  $F_2$  is represented by the dashed line. The  $s=3$  maximum of  $F_3$  is represented by the solid line. Intersections maximize the product  $F_2 F_3$ .

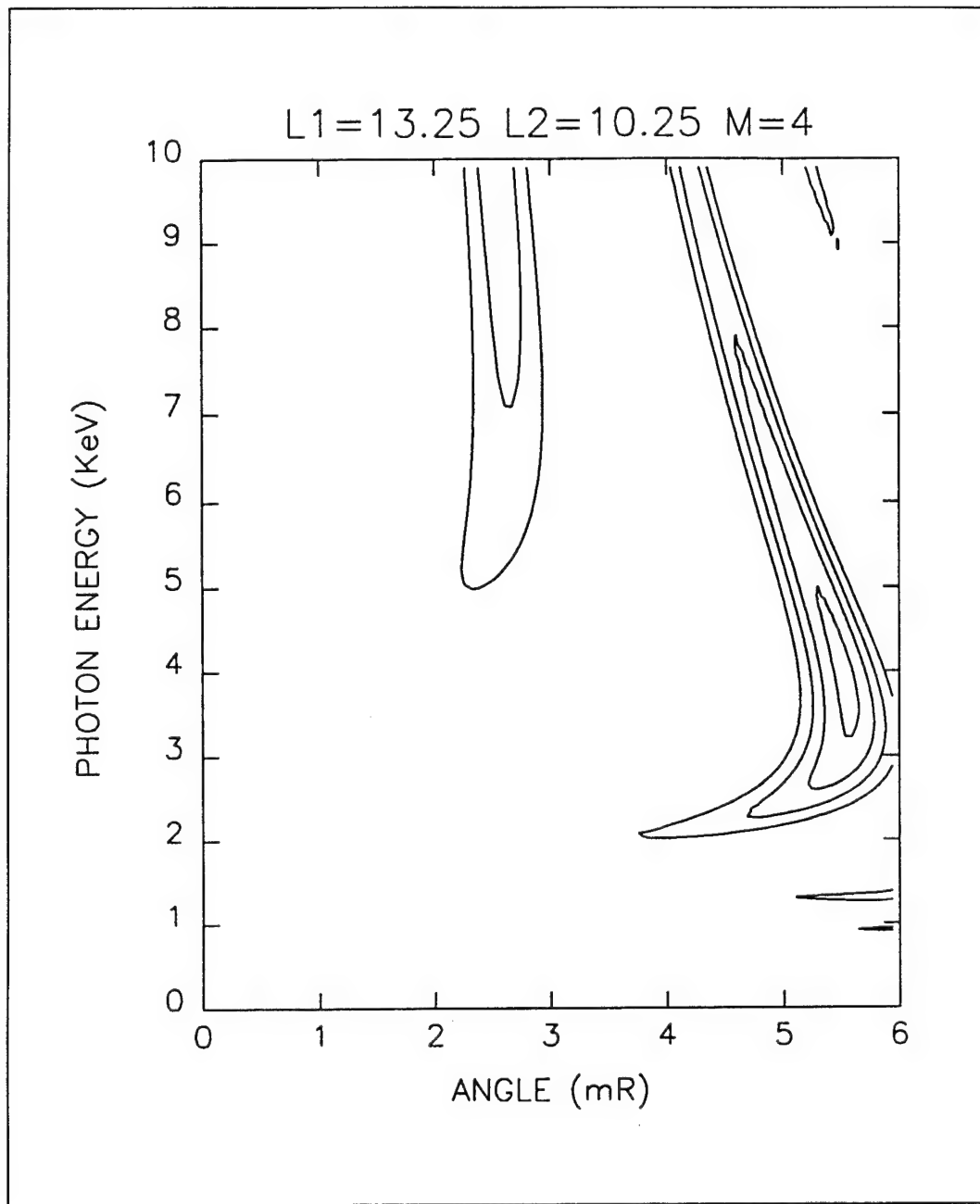


Fig. 31 With  $l_1 = 13.25 \mu\text{m}$ ,  $l_2 = 10.25 \mu\text{m}$ , the radiation pattern for 4 Kapton foils with no absorption is shown.

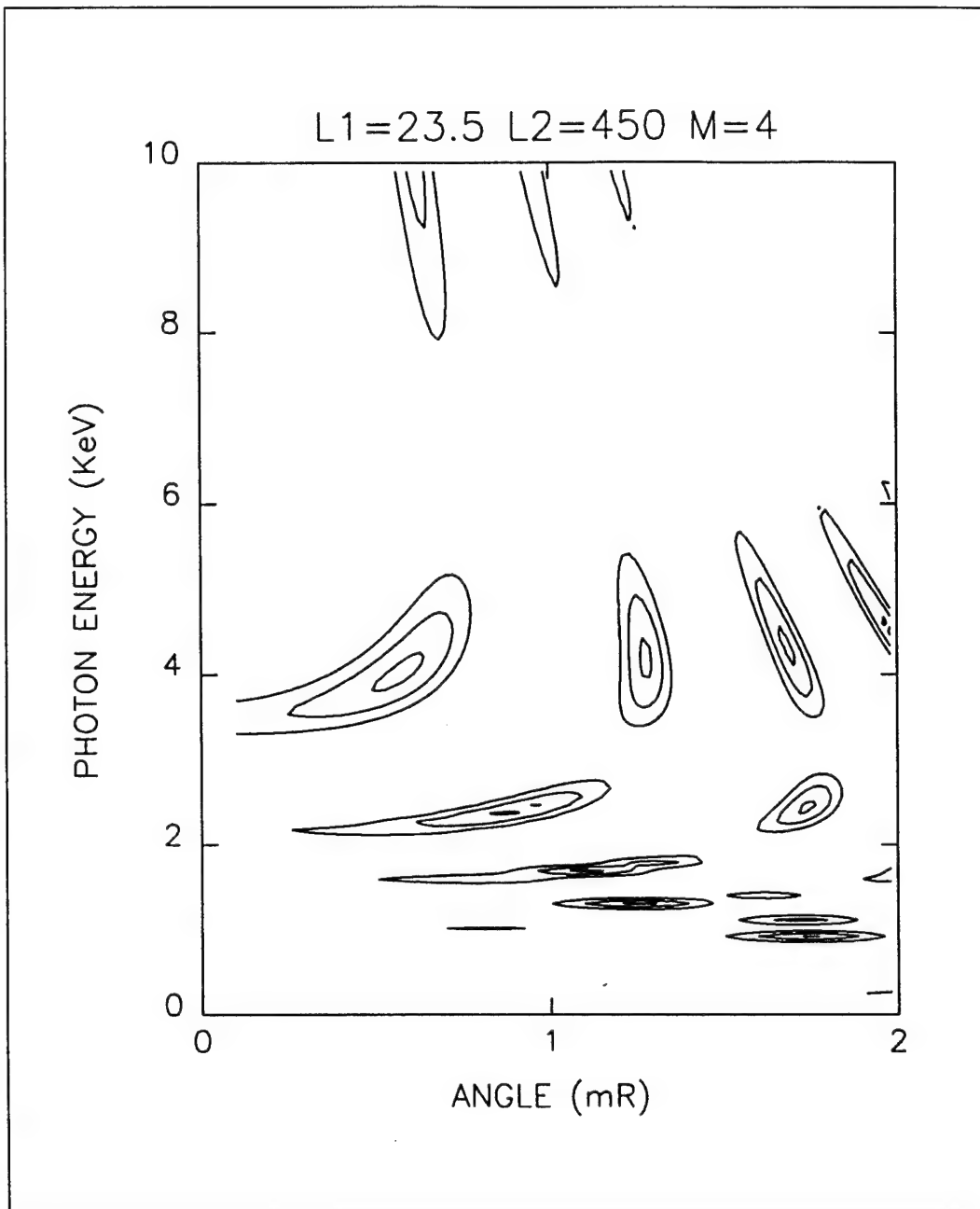


Fig. 32 With  $L_1 = 23.5 \mu\text{m}$ ,  $L_2 = 450 \mu\text{m}$ , the radiation pattern for 4 Kapton foils with no absorption is shown.

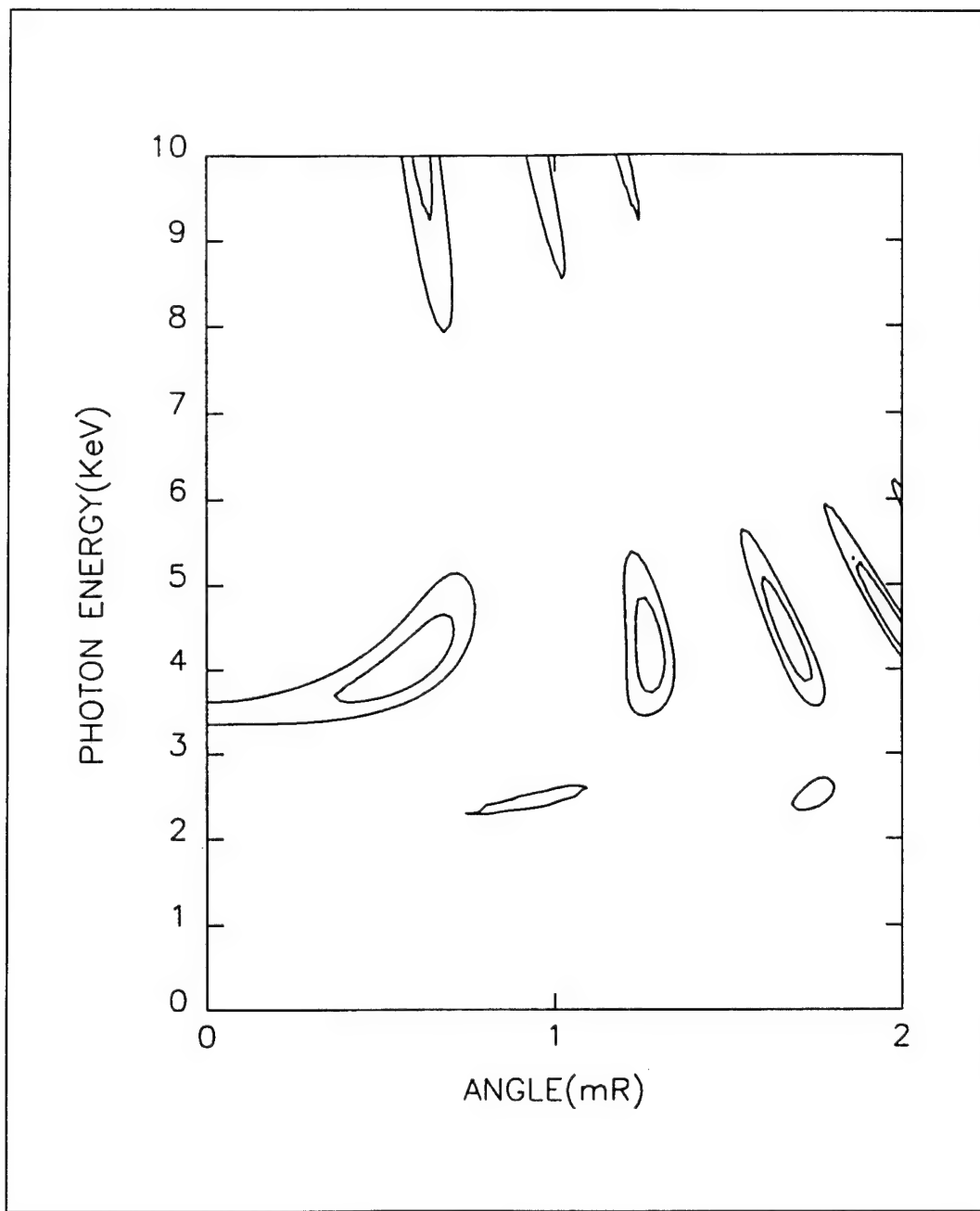


Fig. 33 With  $l_1 = 23.5 \mu\text{m}$ ,  $l_2 = 450 \mu\text{m}$ , the radiation pattern for 4 Kapton foils taking absorption into account is shown. Compare to Fig. 32.

## **VIII. CONCLUSIONS AND FUTURE WORK**

### **A. CONCLUSIONS**

The algorithm developed and used in this thesis is an excellent way to predict the radiation produced by a foil stack. Once a stack is constructed, if precise cell measurements can be made, one can predict the angle and energy of maximum intensity. Since the sizes in the cell are small, manufacturing the foil stack to precise tolerances can be difficult and expensive. In the analysis of the four foil case, the figures show that if randomness is kept to within 10%, the maximum intensity will be above 90% of  $4N^2$ . Taking absorption into account simply lowered the maximum intensity from  $4N^2$ , depending on the absorption constants. Again, randomness up to 10% kept the maximum intensity to within 90% of this new lower value. Increasing the number of foils shows that this range decreases, for eight foils the randomness must be kept to within 5% to keep the maximum intensity above 90% of  $4N^2$ .

The analysis of absorption in foil stacks gives several interesting conclusions. Obviously, absorption is material dependent, having demonstrated materials with both low absorption and high absorption, kapton and aluminum respectively. But, for materials with high absorption, the results show that precision in spacing is more important than precision in foil thickness. This is the opposite of the no or low absorption case and an important consideration in designing foil stacks.

Another conclusion is that the peak is enhanced compared to the lower energy radiation, as a result of the decrease in absorption with increasing energy. The effect is to create an apparent threshold energy at the peak energy, below which radiation is highly absorbed. The value of this apparent threshold is material dependent, but it may be useful in designing detectors.

The last conclusion is the effect of the K edge on the radiation pattern. This result shows this effect can be used to isolate a narrow energy and angle, particularly if some randomness in foil and spacing is incorporated into the design. The technique of

using the K edge to isolate energy is similar to the technique in X-rays of the long known Ross filter where the K edge is used to isolate a particular wavelength.[Ref. 6]

## B. FUTURE WORK

In demonstrating how changing the foil thickness and spacing change the energy and angle of a particular maximum, thicker foils were used. While thicker foils have the obvious effect of increasing the amount of absorption, consideration of multiple electron scattering must be included. For thin foils, multiple electron scattering is a negligible effect. To consider this effect, a Monte Carlo type calculation could be done to simulate the random events.

## **APPENDIX A. ABSORPTION CONSTANTS**

The constants used to determine the linear absorption coefficients for Kapton, Aluminum, and Titanium are listed below. The constants for Kapton and Aluminum[Ref. 4] and Titanium[Ref. 5] were determined using a linear regression of the Photo Absorption vs. energy. The constants for Kapton were determined by using a weighted average of its components.

Absorption Constants

Material	$c_1 [m^{-1}]$	$c_2$
Kapton	$2.9286 \times 10^5$	-2.9238
Aluminum	$4.3544 \times 10^6$	-2.7876
Titanium	$2.547 \times 10^6$	-2.6848
(Above K edge)	$1.7406 \times 10^7$	-2.6014



## APPENDIX B. MAXIMUM INTENSITIES

Values of the maximum intensities for increasing randomness for the both no absorption and absorption in different materials are listed below. The normalized values are divided by  $4N^2$  to make comparisons between different materials. These values were used to create Fig. 14, 19, 23, 24, and 25. Each set of values has been averaged over ten cycles.

Kapton 4 foils No Absorption

% Rand	Variation in Space	Normalized value	Variations in Foil	Normalized value	Variations in Both	Normalized value
0	63.972	1.0	63.972	1.0	63.972	1.0
10	62.406	0.976	61.196	0.957	56.261	0.879
20	58.201	0.910	54.240	0.848	40.593	0.635
30	52.518	0.821	46.392	0.725	28.038	0.438
40	46.718	0.730	39.601	0.619	20.535	0.321

Kapton 8 Foils No Absorption

% Rand	Variations in Spacing			Variations in Foils			Variations in Both		
	Value	Norm	Avg	Value	Norm	Avg	Value	Norm	Avg
0	255.73	1.0	1.0	255.73	1.0	1.0	255.73	1.0	1.0
10	230.61	0.902		226.26	0.885		195.44	0.764	
10	226.88	0.887	0.895	224.07	0.876	0.881	203.20	0.795	0.779
20	190.11	0.743		155.05	0.606		103.33	0.404	
20	179.07	0.700	0.722	166.89	0.653	0.629	94.803	0.371	0.387
30	160.32	0.627		146.50	0.573		63.960	0.250	
30	138.62	0.542	0.585	134.66	0.527	0.550	67.290	0.263	0.257
40	94.378	0.369		88.524	0.346		40.400	0.158	
40	120.72	0.472	0.421	84.254	0.329	0.338	56.065	0.219	0.189

Aluminum 4 Foils with Absorption

% Rand	Variations in Spacing			Variations in Foils			Variations in Both		
	Value	Norm	Avg	Value	Norm	Avg	Value	Norm	Avg
0	45.626	0.713	0.713	45.626	0.713	0.713	45.626	0.713	0.713
10	38.245	0.598		43.999	0.688		36.717	0.574	
10	38.245	0.598	0.598	43.999	0.688	0.688	37.710	0.589	0.582
20	31.344	0.490		38.440	0.601		28.066	0.439	
20	31.344	0.490	0.490	40.367	0.631	0.616	30.442	0.476	0.457
30	23.154	0.362		33.855	0.529		18.883	0.295	
30	23.154	0.362	0.362	37.553	0.587	0.558	19.913	0.311	0.303
40	16.067	0.251		32.209	0.503		16.126	0.252	
40	16.067	0.251	0.251	37.345	0.584	0.543	16.030	0.251	0.252

Kapton 4 Foils with Absorption

% Rand	Variations in Spacing			Variations in Foils			Variations in Both		
	Value	Norm	Avg	Value	Norm	Avg	Value	Norm	Avg
0	61.156	0.956	0.956	61.156	0.956	0.956	61.156	0.956	0.956
10	58.209	0.910		57.953	0.906		56.801	0.888	
10	57.785	0.903	0.907	57.260	0.895	0.899	56.004	0.875	0.882
20	49.687	0.777		48.821	0.763		40.419	0.632	
20	50.784	0.794	0.786	50.256	0.786	0.775	42.417	0.663	0.646
30	40.648	0.635		43.579	0.681		25.022	0.391	
30	38.711	0.605	0.620	41.361	0.647	0.664	25.113	0.393	0.392
40	32.789	0.513		31.848	0.498		22.696	0.355	
40	36.479	0.570	0.542	30.563	0.478	0.488	22.228	0.347	0.351

Titanium 4 Foils with Absorption

% Rand	Variations in Spacing			Variations in Foils			Variations in Both		
	Value	Norm	Avg	Value	Norm	Avg	Value	Norm	Avg
0	44.621	0.696	0.696	44.621	0.696	0.696	44.621	0.696	0.696
10	39.851	0.623		42.289	0.661		39.601	0.619	
10	41.561	0.650	0.637	43.378	0.678	0.670	37.825	0.591	0.605
20	27.028	0.442		40.067	0.626		26.758	0.418	
20	32.899	0.514	0.478	37.370	0.584	0.605	31.805	0.497	0.458
30	28.036	0.438		31.776	0.497		19.044	0.298	
30	30.699	0.480	0.459	28.621	0.447	0.472	16.796	0.263	0.281
40	21.751	0.340		27.019	0.422		17.007	0.256	
40	17.087	0.267	0.304	27.060	0.423	0.423	14.540	0.227	0.242

## APPENDIX C. COMPUTER PROGRAMS

Programs used in calculating the plots of this thesis. The programs are written in IDL and were run on a MicroVAX. The first two programs were written by Dr. J. R. Neighbours, and the rest by CPT Nicholas J. Prins.

Program to calculate the  $r$  vs.  $s$  plots:

```
Print, "***** program TR_E_1.PRO *****"  
;INPUT IS IN KEV AND MICROMETERS HOWEVER, ELECTRON BEAM IS  
;IN MEV  
PN=101  
PPN=5  
I=INDGEN(PPN)  
J=INDGEN(PN)  
E=FLTARR(PN)  
ZS=FLTARR(PPN,PN)  
ZR=FLTARR(PPN,PN)  
R=FLTARR(PPN)  
S=FLTARR(PPN)  
ANGR=FLTARR(PPN,PN)  
ANGS=FLTARR(PPN,PN)  
;  
H=4.12567E-18          ;PLANCK IN KEV SEC  
C=2.997925E14          ;C IN MICROMETERS /SEC  
EB=855                 ;ELECTRON BEAM ENERGY (MEV)  
L1=7.5                  ;FOIL THICKNESS IN MICROMETERS  
L2=169                  ;FOIL SPACING IN MICROMETERS  
EP=25.0E-3               ;FOIL PLASMA ENERGY IN KEV  
SZERO=1                 ;AN ODD INTEGER  
RZERO=1                 ;AN INTRGER  
E0=0.5                  ;BEGINNING PHOTON ENERGY  
INTERVAL=9.5             ;PHOTON ENERGY INTERVAL IN KEV  
DE=INTERVAL/PN  
DI=1.0  
;  
GAM=EB/0.511             ;GAMMA  
L=L1+L2  
FOR I=0,(PPN-1) DO BEGIN  
  S(I)=SZERO+2.0*I  
  R(I)=RZERO+I
```

```

FOR J=0,(PN-1) DO BEGIN
E(J)=E0+J*DE
ZS(I,J)=-1/GAM^2-(EP/E(J))^2+S(I)*(H*C)/(L1*E(J))
ZR(I,J)=-1/GAM^2-(L1/L)*(EP/E(J))^2+2.0*R(I)*H*C/(E(J)*L)
ANGR(I,J)=1000*SQRT(ZR(I,J))
ANGS(I,J)=1000*SQRT(ZS(I,J))
ENDFOR
    ENDFOR
;-----
SET_PLOT,1
!TYPE=28
!FANCY=3
!XMAX=2.0
!XMIN=0
!YMAX=10.0
!YMIN=0
!XTICKS=2
!YTICKS=5
!PSYM=0
!XTITLE='ANGLE (mR)
!YTITLE=' PHOTON ENERGY (KeV)'
!MTITLE='L1=7.5 L2=169'
!LINETYPE=0
PLOT,ANGR(0,*),E
!LINETYPE=1
OPLOT,ANGS(0,*),E
FOR I=1,(PPN-1) DO BEGIN
    !LINETYPE=0
    OPLOT,ANGR(I,*),E
    !LINETYPE=1
    OPLOT,ANGS(I,*),E
ENDFOR
!LINETYPE=0
STOP,"CONTINUE FOR TEK PLOT" ;-----
SET_PLOT,'4014'
!TYPE=28
!FANCY=3
!LINETYPE=0
!PSYM=0
TITLE='L1_7_L2_169_E_VS_ANG' ; FILENAME OF PLOT
OPENW,5,TITLE+'_TEK.PLT/NONE'
PLOT_TO,-5
SET_VIEWPORT,0.25,0.75,0.1,0.9

```

```

!XTITLE='ANGLE (mR)'
!YTITLE=' PHOTON ENERGY (KeV)'
!MTITLE='L1=7.5 L2=169'
!XMAX=2.0
!XMIN=0
!YMAX=10.0
!YMIN=0
!XTICKS=2
!YTICKS=5
!LINETYPE=0
PLOT,ANGR(0,*),E
!LINETYPE=1
OPLOT,ANGS(0,*),E
FOR I=1,(PPN-1) DO BEGIN
  !LINETYPE=0
  OPLOT,ANGR(I,*),E
  !LINETYPE=1
  OPLOT,ANGS(I,*),E
ENDFOR
CLOSE,5
PLOT_TO,0
PRINT,"=====END=====END=====END===="
END

```

Program to calculate the contour plots:

```

Print, "***** program TR_E_1_CONT.PRO *****"
;INPUT IS IN KEV AND MICROMETERS HOWEVER, ELECTRON BEAM IS
;IN MEV THIS PROGRAM INCLUDES M THE NUMBER OF FOILS TO MAKE
; A CONTOUR PLOT
PN=101
PPN=5
I=INDGEN(PPN)
J=INDGEN(PN)
E=FLTARR(PN)
THET=FLTARR(PN)
BRAK=FLTARR(PPN,PN)
BRAK2=FLTARR(PPN,PN)
Y=FLTARR(PPN,PN)
X=FLTARR(PPN,PN)
F2=FLTARR(PPN,PN)
F3=FLTARR(PPN,PN)
;-----

```

```

H=4.12567E-18 ;PLANCK IN KEV SEC
C=2.997925E14 ;C IN MICROMETERS /SEC
EB=855 ;ELECTRON BEAM ENERGY (MEV)
L1=7.5 ;FOIL THICKNESS IN MICROMETERS
L2=169 ;FOIL SPACING IN MICROMETERS
EP=25.0E-3 ;FOIL PLASMA ENERGY IN KEV
M=8
E0=0.5 ;BEGINNING PHOTON ENERGY
INTERVAL=9.5 ;PHOTON ENERGY INTERVAL IN KEV
DE=INTERVAL/PN
THET0=0.10 ;INITIAL THETA VALUE
THETINTER=1.90 ;THETA INTERVAL IN MILLIRADIANS
DTHET=THETINTER/PPN
;-----
GAM=EB/0.511 ;GAMMA
CONST1=!PI/(H*C*2)
L=L1+L2
FOR I=0,(PPN-1) DO BEGIN
    THET(I)=(THET0+I*DTHET)/1000
FOR J=0, (PN-1) DO BEGIN
    E(J)=E0+J*DE
    BRAK(I,J)=1/GAM^2+THET(I)^2+(EP/E(J))^2
    Y(I,J)=CONST1*L1*E(J)*BRAK(I,J)
    F2(I,J)=4*(SIN(Y(I,J)))^2
    BRAK2(I,J)=L*(1/GAM^2+THET(I)^2+L1*(EP/E(J))^2
    X(I,J)=CONST1*E(J)*BRAK2(I,J)
    F3(I,J)=(SIN(M*X(I,J))/SIN(X(I,J)))^2
ENDFOR
    ENDFOR
;-----
SET_PLOT,1
!TYPE=28
!FANCY=3
!XMAX=2.0
!XMIN=0
!YMAX=10.0
!YMIN=0
!XTICKS=2
!YTICKS=5
!PSYM=0
!XTITLE='ANGLE (mR)'
!YTITLE=' PHOTON ENERGY (KeV)'
!MTITLE='L1=7.5 L2=169 M=4'

```

```

!LINETYPE=0
!NORMALCONT=2 ;CONTOURS NOT LABELED
CONTOURXY,F2*F3,THET*1000,E,0,30,10
STOP,"CONTINUE FOR TEK PLOT";-----
SET_PLOT,'4014'
!TYPE=28
!FANCY=3
!LINETYPE=0
!PSYM=0
TITLE='L1_7_L2_169_CONT' ; FILENAME OF PLOT
OPENW,5,TITLE+'_TEK.PLT/NONE'
PLOT_TO,-5
SET_VIEWPORT,0.25,0.75,0.1,0.9
!XTITLE='ANGLE (mR)'
!YTITLE=' PHOTON ENERGY (KeV)'
!MTITLE='L1=7.5 L2=169 M=4'
!XMAX=2.0
!XMIN=0
!YMAX=10.0
!YMIN=0
!XTICKS=2
!YTICKS=5
!LINETYPE=0
!NORMALCONT=2 ;CONTOURS NOT LABELED
CONTOURXY,F2*F3,THET*1000,E,0,30,10
CLOSE,5
PLOT_TO,0
PRINT,"=====END=====END=====END===="
END

```

Program to verify the summation for Eq. 15:

```

PRINT,***** PROGRAM F2F3INT1.PRO *****
;GIVES THE RESULTING F2*F3 FOR N FOILS WHEN THICKNESS AND SPACING
;VARY. THE RESULT OF F2*F3 IS FROM THE SUMMATION
PN=201
PPN=3
N=4
I=INDGEN(PPN)
J=INDGEN(PN)
R=FLTARR(PN)
S=FLTARR(PN)
ROA=FLTARR(N+3)

```

```

ROB=FLRARR(N+3)
A=FLTARR(N+3)
DELB=FLTARR(4*PN)
F23=FLTARR(PN,PN)
Z1=FLTARR(PN,PN)
Z2=FLTARR(PN,PN)
E=FLTARR(PN)
ANG=FLTARR(PN)
F2F3=FLTARR(N+3)

;-----  

H=4.12567E-18          ;PLANCK IN KEV SEC
C=2.997925E14          ;C IN MICROMETERS /SEC
EB=855                  ; ELECTRON BEAM ENERGY (MEV)
L1=7.5                  ;FOIL THICKNESS IN MICROMETERS
L2=169                  ;FOIL SPACING IN MICROMETERS
EP=25.0E-3               ;FOIL PLASMA ENERGY IN KEV
PI=3.14159
E(0)=0.001
ANG(0)=0.0
;-----ENG AND ANG VARY
FOR I=1,100 DO BEGIN
    E(I)=I/10.0
    ANG(I)=(I/(100/2.0))*1E-3
ENDFOR
;-----CALC Z1&Z2
GAM=EB/0.511            ;GAMMA
FOR I=0,100 DO BEGIN
    FOR J=0,100 DO BEGIN
        Z1(I,J)=2*C*H/(PI*E(J)*(1/GAM^2+(EP/E(J))^2+ANG(I)^2))
        Z2(I,J)=2*C*H/(PI*E(J)*(1/GAM^2+ANG(I)^2))
    ENDFOR
ENDFOR
;-----CALC DELTA IN SPACING
AN=0
BN=0
FOR K=1,N DO BEGIN
    ROA(K)=AN
    ROB(K)=BN
ENDFOR
;-----FIND F2*F3
FOR I=0,100 DO BEGIN
    FOR J=0,100 DO BEGIN
;-----CALC AM

```

```

FOR M=0,N DO BEGIN
    ADUM=0
    BDUM=0
    FOR K=(M+2),N DO BEGIN
        ADUM=ADUM+(ROA(K)/L1)+1
        BDUM=BDUM+(ROB(K-1)/L2)+1
    ENDFOR
    A(M)=-2*L1*ADUM/Z1(I,J)-2*L2*BDUM/Z2(I,J)
ENDFOR
;-----CALC F2*F3
FSUM=COMPLEX(0,0)
FOR M=0,(N-1) DO BEGIN
    ROM=(-1/Z1(I,J))*L1
    FR=2*SIN(A(M)+ROM)*SIN(ROM)
    FI=-2*SIN(ROM)*COS(A(M)+ROM)
    F=COMPLEX(FR,FI)
    FSUM=FSUM+F
ENDFOR
F23(I,J)=(FSUM*CONJ(FSUM))
ENDFOR
ENDFOR
;-----
SET_PLOT,1
!TYPE=28
!FANCY=3
!XMAX=2.0
!XMIN=0
!YMAX=10.0
!YMIN=0
!XTICKS=2
!YTICKS=5
!PSYM=0
!LINETYPE=0
!NORMALCONT=2 ;CONTOURS NOT LABELED
CONTOURXY,F2*F3,ANG*1000,E,0,30,10
STOP,"CONTINUE FOR TEK PLOT";-----
SET_PLOT,'4014'
!TYPE=28
!FANCY=3
!LINETYPE=0
!PSYM=0
TITLE='F2F3INT_1' ; FILENAME OF PLOT
OPENW,5,TITLE+'_TEK.PLT/NONE'

```

```

PLOT_TO,-5
SET_VIEWPORT,0.25,0.75,0.1,0.9
!XTITLE='ANGLE (mR)'
!YTITLE=' PHOTON ENERGY (KeV)'
!MTITLE='F2F3 FROM SUMMATION'
!XMAX=2.0
!XMIN=0
!YMAX=10.0
!YMIN=0
!XTICKS=2
!YTICKS=5
!LINETYPE=0
!NORMALCONT=2 ;CONTOURS NOT LABELED
CONTOURXY,F2*F3,ANG*1000,E,0,30,10
CLOSE,5
PLOT_TO,0
PRINT,"=====END=====END====="
END

```

Program to use randomness and average over n cycles:

```

PRINT,'***** PROGRAM F2F3INT7.PRO *****'
;GIVES THE RESULTING F2*F3 FOR N FOILS WHEN THICKNESS AND SPACING
;VARY BY A RANDOM AMOUNT. THE RESULT OF F2*F3 IS CALCULATED FOR
; R CYCLES, SUMMED AVERAGED AND CONTOURED.
PN=101
R=10
N=4
A=FLTARR(N+3)
F23=FLTARR(PN,PN)
Z1=FLTARR(PN,PN)
Z2=FLTARR(PN,PN)
E=FLTARR(PN)
ANG=FLTARR(PN)
F2F3=FLTARR(PN,PN)
TH=FLTARR(N+3)
SP=FLTARR(N+3)
ASM=FLTARR(N+3)
BSM=FLTARR(N+3)
F23AV=FLTARR(PN,PN)
;-----
H=4.12567E-18 ;PLANCK IN KEV SEC
C=2.997925E14 ;C IN MICROMETERS /SEC

```

```

EB=855 ; ELECTRON BEAM ENERGY (MEV)
L1=7.5 ; FOIL THICKNESS IN MICROMETERS
L2=169 ; FOIL SPACING IN MICROMETERS
EP=25.0E-3 ; FOIL PLASMA ENERGY IN KEV
PI=3.14159
DELTH=0.1*L1 ; VARIATION IN THICKNESS
DELSP=0.1*L2 ; VARIATION IN SPACING
;-----ENG AND ANG VARY
FOR I=1,100 DO BEGIN
    E(I)=I/10.0
    ANG(I)=(I/(100/2.0))*1E-3
ENDFOR
E(0)=0.001
;-----CALC Z1&Z2
GAM=EB/0.511 ;GAMMA
FOR I=0,100 DO BEGIN
    FOR J=0,100 DO BEGIN
        Z1(I,J)=2*C*H/(PI*E(J)*(1/GAM^2+(EP/E(J))^2+ANG(I)^2))
        Z2(I,J)=2*C*H/(PI*E(J)*(1/GAM^2+ANG(I)^2))
    ENDFOR
ENDFOR
FOR T=0,R-1 DO BEGIN ;BEGIN R CYCLES
;-----CALC DELTA IN SPACING
FOR I=0,N DO BEGIN
    TH(I)=L1
    SP(I)=L2
ENDFOR
SP=SP+DELSP*RANDOMN(S,N+3)
TH=TH+DELTH*RANDOMN(S,N+3)
SP(N:N+2)=0.0
TH(N+1:N+2)=0.0
SP(0)=0.0
TH(0)=0.0
;-----FIND F2*F3
FOR I=0,100 DO BEGIN
    FOR J=0,100 DO BEGIN
;-----CALC AM
FOR M=0,N DO BEGIN
    ASUM=0.0
    BSUM=0.0
    FOR P=(M+2),N DO BEGIN
        ASUM=ASUM+TH(P)
        BDUM=BDUM+SP(P-1)

```

```

        ENDFOR
ASM(M)=ASUM
BSM(M)=BSUM
A(M)=-2*ASM(M)/Z1(I,J)-2*BSM(M)/Z2(I,J)
ENDFOR
;-----CALC F2*F3
FSUM=COMPLEX(0,0)
FOR M=0,(N-1) DO BEGIN
    ROM=(-TH(M+1)/Z1(I,J)
    FR=2*SIN(A(M)+ROM)*SIN(ROM)
    FI=-2*SIN(ROM)*COS(A(M)+ROM)
    F=COMPLEX(FR,FI)
    FSUM=FSUM+F
ENDFOR
F23(I,J)=(FSUM*CONJ(FSUM))
ENDFOR
ENDFOR
F2F3=F2F3+F23
ENDFOR
F23AV=F2F3/10.0
;-----
PRINT,MAX(F23AV)
SET_PLOT,1
!TYPE=28
!FANCY=3
!XMAX=2.0
!XMIN=0
!YMAX=10.0
!YMIN=0
!XTICKS=2
!YTICKS=5
!PSYM=0
!LINETYPE=0
!NORMALCONT=2 ;CONTOURS NOT LABELED
CONTOURXY,F23AV,ANG*1000,E,0,30,10
STOP,"CONTINUE FOR TEK PLOT";-----
SET_PLOT,'4014'
!TYPE=28
!FANCY=3
!LINETYPE=0
!PSYM=0
TITLE='F2F3INT7_1' ;FILENAME OF PLOT
OPENW,5,TITLE+'_TEK.PLT/NONE'

```

```

PLOT_TO,-5
SET_VIEWPORT,0.25,0.75,0.1,0.9
!XTITLE='ANGLE (mR)'
!YTITLE=' PHOTON ENERGY (KeV)'
!MTITLE='10% RANDOM KAPTON 4 FOILS
!XMAX=2.0
!XMIN=0
!YMAX=10.0
!YMIN=0
!XTICKS=2
!YTICKS=5
!LINETYPE=0
!NORMALCONT=2 ;CONTOURS NOT LABELED
CONTOURXY,F23AV,ANG*1000,E,0,30,10
CLOSE,5
PLOT_TO,0
PRINT,"-----END-----END-----"
END

```

Program to take absorption into account:

```

PRINT,'***** PROGRAM ABSORB3.PRO *****'
;COPY OF F2F3INT7.PRO WHICH IS MODIFIED TO TAKE ABSORPTION IN
;EFFECT GIVES THE RESULTING F2*F3 FOR N FOILS WHEN THICKNESS AND
;SPACING VARY BY A RANDOM AMOUNT. THE RESULT OF F2*F3 IS
;CALCULATED FOR ; R CYCLES, SUMMED AVERAGED AND CONTOURED.
PN=101
R=10
N=4
A=FLTARR(N+3)
F23=FLTARR(PN,PN)
Z1=FLTARR(PN,PN)
Z2=FLTARR(PN,PN)
E=FLTARR(PN)
ANG=FLTARR(PN)
F2F3=FLTARR(PN,PN)
TH=FLTARR(N+3)
SP=FLTARR(N+3)
ASM=FLTARR(N+3)
BSM=FLTARR(N+3)
F23AV=FLTARR(PN,PN)
MU=FLTARR(PN)
;-----

```

```

H=4.12567E-18          ;PLANCK IN KEV SEC
C=2.997925E14          ;C IN MICROMETERS /SEC
EB=855                  ; ELECTRON BEAM ENERGY (MEV)
L1=7.5                  ;FOIL THICKNESS IN MICROMETERS
L2=169                  ;FOIL SPACING IN MICROMETERS
EP=25.0E-3               ;FOIL PLASMA ENERGY IN KEV
PI=3.14159
DELTH=0.1*L1             ;VARIATION IN THICKNESS
DELSP=0.1*L2             ;VARIATION IN SPACING
C1=.29286                ;ABSORPTION CONSTANT FOR KAPTON
C2=-2.9238               ;OTHER ABSORPTION CONSTANT
;-----ENG AND ANG VARY
FOR I=1,100 DO BEGIN
    E(I)=I/10.0
    ANG(I)=(I/(100/2.0))*1E-3
ENDFOR
E(0)=0.001
FOR I=0,100 DO BEGIN
    MU(I)=C1*E(I)^C2
ENDFOR
;-----CALC Z1&Z2
GAM=EB/0.511             ;GAMMA
FOR I=0,100 DO BEGIN
    FOR J=0,100 DO BEGIN
        Z1(I,J)=2*C*H/(PI*E(J)*(1/GAM^2+(EP/E(J))^2+ANG(I)^2))
        Z2(I,J)=2*C*H/(PI*E(J)*(1/GAM^2+ANG(I)^2))
    ENDFOR
ENDFOR
FOR T=0,R-1 DO BEGIN      ;BEGIN R CYCLES
;-----CALC DELTA IN SPACING
FOR I=0,N DO BEGIN
    TH(I)=L1
    SP(I)=L2
ENDFOR
SP=SP+DELSP*RANDOMN(S,N+3)
TH=TH+DELTH*RANDOMN(S,N+3)
SP(N:N+2)=0.0
TH(N+1:N+2)=0.0
SP(0)=0.0
TH(0)=0.0
;-----FIND F2*F3
FOR I=0,100 DO BEGIN
    FOR J=0,100 DO BEGIN

```

```

;-----CALC AM
FOR M=0,N DO BEGIN
    ASUM=0.0
    BSUM=0.0
    FOR P=(M+2),N DO BEGIN
        ASUM=ASUM+TH(P)
        BDUM=BDUM+SP(P-1)
    ENDFOR
    ASM(M)=ASUM
    BSM(M)=BSUM
    A(M)=-2*ASM(M)/Z1(I,J)-2*BSM(M)/Z2(I,J)
ENDFOR
;-----CALC F2*F3
FSUM=COMPLEX(0,0)
FOR M=0,(N-1) DO BEGIN
    ROM=(-TH(M+1))/Z1(I,J)
    FR=2*SIN(A(M)+ROM)*SIN(ROM)
    FI=-2*SIN(ROM)*COS(A(M)+ROM)
    F=COMPLEX(FR,FI)
    FSUM=FSUM+F*EXP(-2MU(J)*ASM(M)/Z1(I,J))
ENDFOR
F23(I,J)=(FSUM*CONJ(FSUM))
ENDFOR
ENDFOR
F2F3=F2F3+F23
ENDFOR
F23AV=F2F3/(1.0*R)
;-----PRINT,MAX(F23AV)
SET_PLOT,1
!TYPE=28
!FANCY=3
!XMAX=2.0
!XMIN=0
!YMAX=10.0
!YMIN=0
!XTICKS=2
!YTICKS=5
!PSYM=0
!LINETYPE=0
!NORMALCONT=2           ;CONTOURS NOT LABELED
CONTOURXY,F23AV,ANG*1000,E,0,30,10
STOP,"CONTINUE FOR TEK PLOT";-----
```

```

SET_PLOT,'4014'
!TYPE=28
!FANCY=3
!LINETYPE=0
!PSYM=0
TITLE='ABSORB3_1' ; FILENAME OF PLOT
OPENW,5,TITLE+'_TEK.PLT/NONE'
PLOT_TO,-5
SET_VIEWPORT,0.25,0.75,0.1,0.9
!XTITLE='ANGLE (mR)'
!YTITLE=' PHOTON ENERGY (KeV)'
!MTITLE='10% RAND ABSORB KAPTON 4 FOILS
!XMAX=2.0
!XMIN=0
!YMAX=10.0
!YMIN=0
!XTICKS=2
!YTICKS=5
!LINETYPE=0
!NORMALCONT=2           ;CONTOURS NOT LABELED
CONTOURXY,F23AV,ANG*1000,E,0,30,10
CLOSE,5
PLOT_TO,0
PRINT,"=====END=====END=====END===="
END

```

Program to find the angle and energy of the  $r = 2, s = 3$  intersection:

```

Print, "***** program L1INT.PRO *****"
;INPUT IS IN KEV AND MICROMETERS HOWEVER, ELECTRON BEAM IS
;IN MEV CALCULATES R=2,S=3 INTERSECTIONS AS L1 VARIES AND L2 IS
;HELD CONSTANT
PN=101
PPN=5
I=INDGEN(PPN)
J=INDGEN(PN)
E=FLTARR(PN)
ZS=FLTARR(PPN,PN)
ZR=FLTARR(PPN,PN)
R=FLTARR(PPN)
S=FLTARR(PPN)
ANGR=FLTARR(PPN,PN)
ANGS=FLTARR(PPN,PN)

```

```

ABOVE=FLTARR(20*PN)
B=FLTARR(PN)
D=FLTARR(PN)
ANGINT=FLTARR(2*PN)
ENGINT=FLTARR(2*PN)
AI=FLTARR(PN)
EI=FLTARR(PN)
;-----
H=4.12567E-18          ;PLANCK IN KEV SEC
C=2.997925E14          ;C IN MICROMETERS /SEC
EB=855                  ;ELECTRON BEAM ENERGY (MEV)
L2=169                  ;FOIL SPACING IN MICROMETERS
EP=25.0E-3               ;FOIL PLASMA ENERGY IN KEV
SZERO=1                 ;AN ODD INTEGER
RZERO=1                 ;AN INTRGER
E0=0.5                  ;BEGINNING PHOTON ENERGY
INTERVAL=9.5             ;PHOTON ENERGY INTERVAL IN KEV
DE=INTERVAL/PN
DI=1.0
;-----
GAM=EB/0.511            ;GAMMA
FOR L1=5,100 DO BEGIN   ;FOIL THICKNESS IN MICROMETERS
L=L1+L2
I=1
S(I)=SZERO+2.0*I
R(I)=RZERO+I
FOR J=0,(PN-1) DO BEGIN
E(J)=E0+J*DE
ZS(I,J)=-1/GAM^2-(EP/E(J))^2+S(I)*(H*C)/(L1*E(J))
ZR(I,J)=-1/GAM^2-(L1/L)*(EP/E(J))^2+2.0*R(I)*H*C/(E(J)*L)
ANGR(I,J)=1000*SQRT(ZR(I,J))
ANGS(I,J)=1000*SQRT(ZS(I,J))
ENDFOR
B=ANGR(1,*)              ;R=2
D=ANGS(1,*)              ;S=3
ABOVE=B(WHERE(B LT D))
ANGINT(L1)=ABOVE(1)
EENG=PN-SIZE(ABOVE)
ENGINT(L1)=E(EENG(1))
ENDFOR
AI=ANGINT(WHERE(ANGINT GT 0))
EI=ENGINT(WHERE (ENGINT GT 0))
;-----

```

```

SET_PLOT,1
!TYPE=28
!FANCY=3
!XMAX=6.0
!XMIN=0
!YMAX=40.0
!YMIN=0
!XTICKS=6
!YTICKS=8
!PSYM=0
!LINETYPE=0
PLOT,AI,EI
STOP,"CONTINUE FOR TEK PLOT";-----
SET_PLOT,'4014'
!TYPE=28
!FANCY=3
!LINETYPE=0
!PSYM=0
TITLE='L1_VARIES'; FILENAME OF PLOT
OPENW,5,TITLE+'_TEK.PLT/NONE'
PLOT_TO,-5
SET_VIEWPORT,0.25,0.75,0.1,0.9
!XTITLE='ANGLE (mR)'
!YTITLE=' PHOTON ENERGY (KeV)'
!MTITLE='L1 VARIE FROM 5 TO 100'
!XMAX=6.0
!XMIN=0
!YMAX=40.0
!YMIN=0
!XTICKS=6
!YTICKS=8
!LINETYPE=0
PLOT,AI,EI
CLOSE,5
PLOT_TO,0
PRINT,"=====END=====END=====END===="
END

```

## LIST OF REFERENCES

1. M.A.Piestrup, D.G.Boyers, C.I.Pincus, G.D.Hallewell, M.J.Moran, D.M.Skopik, R.M.Silzer, X.K.Marauyama, D.D.Snyder, G.B.Rothbart, *Observation of soft x-ray spatial coherence from resonance transition radiation*, Phys. Rev. A **45**, 1183-1185 (1992).
2. J.R.Neighbours, F.R.Buskirk, H.J.Hartmann, *Calculation of coherent effects in x-ray transition radiation produced by relativistic electrons*, J. Appl. Phys. **75**, 7200-7202 (1994).
3. G.M.Garibyan, L.A.Gevorgyan, C.Yang, *X-ray transition radiation produced in an irregular medium*, Sov. Phys. JETP **39**, 265-266 (1974).
4. H.J.Hartmann, *Aufbau eines Detektorsystems zum Nachweis von Übergangsstrahlung*, Ph.D. Dissertation, Institut für Physik, Johannes Gutenberg-Universität, Mainz, Germany, p. 48-49, February, 1992.
5. E.Storm, H.I.Israel, *Photon cross sections from 1 keV to 100 MeV for elements Z=1 to Z=100*, Nuclear Data Tables, A7:565-681, 1970.
6. P.A.Ross, J.O.S.A. and R.S.I., U.S.A. **16**, 433 (1928).



## INITIAL DISTRIBUTION LIST

1. Defense Technical Information Center.....2  
Cameron Station  
Alexandria, Virginia 22304-61545
2. Library, Code 52.....2  
Naval Postgraduate School  
Monterey, California 93943-5101
3. Professor John Neighbours.....2  
Physics Department, Code PH/NB  
Naval Postgraduate School  
Monterey, California 93943-5002
4. Professor Fred Buskirk.....2  
Physics Department, Code PH/FB  
Naval Postgraduate School  
Monterey, California 93943-5002
5. Professor X. K. Maruyama.....1  
Physics Department, Code PH/MA  
Naval Postgraduate School  
Monterey, California 93943-5002
6. Professor Thomas Walcher.....1  
Institut für Kernphysik  
Universität Mainz  
Becherweg 45  
D 55099 Mainz 1
7. Professor Hartmut Backe.....1  
Institut für Kernphysik  
Universität Mainz  
Becherweg 45  
D 55099 Mainz 1
8. Dr. M. A. Piestrup.....1  
Adelphi Technology  
2181 Park Blvd  
Palo Alto, California 94306

9. Captain Nicholas Prins,USA. ....1  
Department of Physics  
West Point, New York 10996-5000